Chapter 1 Introduction

Improving antenna characteristics such as gain, input impedance, bandwidth, and size has always been the goal of antenna engineers. It is important for the antenna engineer to have the latest tools to effectively design antennas that meet the given specifications. Optimization techniques are used to either synthesize an antenna from given radiation characteristics or simply improve existing antenna designs. Search routines that utilize numerical methods to provide radiation properties of antennas generally consume a considerable amount of time. Therefore, a great deal of work has been devoted to achieving optimization routines that rapidly and accurately search out an optimum solution.

Recently, a unique optimization scheme based on *genetic algorithms* (GA) has been used to solve a number of electromagnetic problems. The genetic algorithm is a robust, stochastic search method that models its processes after the principles of natural selection and evolution [1]. These genetic algorithms are very useful for finding optimum antenna designs that maximize or minimize certain radiation properties. The GA provides optimal solutions by successively creating populations that improve over many generations. Selecting, mating and mutating the previous population each creates a new generation. This process continues until the population converges to a single optimal solution.

The selection process is based upon the rating of each member relative to the population. This rating is done by fitness testing of each individual. The fitness value can be the gain, axial ratio, input impedance, size, sidelobe level or any combination thereof. This fitness value is received from some type of numerical code that can provide the radiation characteristics of the antenna. A method of moment code, called NEC2 [2], is used in this thesis as a fitness function from which the fitness value is obtained.

In this thesis, the aim is to optimize the helical antenna using genetic algorithms. The helical antenna provides circular polarization and relatively constant gain and input impedance over a wide frequency range when operating in the axial mode. There are many variations of the helix that have been studied to improve the axial ratio, bandwidth, gain, voltage standing-wave ratio (VSWR) and size. These variations alter the envelope that the helix is contained in. This thesis will attempt to optimize the shape of the helix by altering the envelope as well as the pitch angle. The GA will optimize a unique combination of the gain and bandwidth of the helical antenna. It is shown that the GA-optimized helix provides a lower axial-ratio over a wider bandwidth, a flatter input impedance characteristic, and slightly higher gain than the conventional helix.

Chapter 2 presents some background information on genetic algorithms and their applications to antenna problems. The theory of the genetic algorithm is discussed in chapter 3. In this chapter, various ways of setting-up the GA and some recommendations are provided. An example is given to illustrate the processes involved in the genetic algorithm. Also, a double-vee dipole antenna is optimized using GA and compared to a previous work done by Patwari and Safaai-Jazi [3], in order to demonstrate its accuracy and efficiency. It is shown that the GA is far superior to any brute-force systematic search method. Chapter 4 reviews the conventional helical antenna and its variations. This chapter provides a basic understanding of the operation and performance of the helical antenna. Also, a proof of the correct setup of NEC2 for the analysis of helical antenna is provided. Chapter 5 presents the setup and optimization of the helical antenna using the genetic algorithm. Computed results for far-field radiation patterns gain, axial ratio, input impedance, bandwidth, and beamwidth are presented in this chapter. The measurement of the GA-optimized helical antenna is addressed in Chapter 6. Measured results for radiation patterns and axial-ratio are obtained and compared with the computed results. Chapter 7 summarized the conclusions of this research and points out directions for further investigations.

Chapter 2 Introduction to Genetic Algorithms

This chapter is presented as a brief introduction to genetic algorithms. Section 2.1 overviews the principles and background behind the ideas underlying the genetic algorithm. These evolutionary principles are key to the search method employed by the genetic algorithm. Section 2.2 provides examples for the applications of genetic algorithms to antenna problems.

2.1 The Genetic Algorithm

There are many problems in electrical engineering for which analytical solutions do not exist. In fact, most practical electromagnetic problems are nonlinear and non-differentiable. These problems require engineers and scientists to employ numerical methods. These methods provide no insight into the global optimum solution of the problem. Thus, the numerical solvers resort to marching parameters up and down until a global optimum is obtained. These brute-force methods are time consuming and unintuitive. Genetic algorithms stochastically evolve a population towards a solution using the concepts of survival of the fittest. These algorithms allow the global optimum, which is the goal of all optimization techniques, to be attained far faster than the traditional brute-force techniques.

In the 1970s, a unique optimization technique developed by information and computer scientists proved to be successful for finding converging solutions for highly non-linear and multi-parameter equations. This technique is based on genetic algorithms that have proven to be powerful optimizers in many different areas of research. J. Holland [1] pioneered much of the early work on genetic algorithms. Many authors since then have contributed a wealth of knowledge to the study and applications of genetic algorithms (GAs). A definitive work, completed by D. Goldberg [4] in 1989, is currently the leading textbook of choice for GAs study.

The concepts behind GAs are motivated by Darwin's [5] theory of descent. This *original optimization scheme* based on Darwin's theory is used to solve certain types of non-differentiable problems. The genetic algorithm mimics the evolutionary notion of survival of the fittest. As the population develops through generations of individuals, the overall fitness of the group increases. If the fitness of particular individuals is not competitive enough for survival, they are doomed to die off and their genetic material is removed from the population.

Each individual in the population is defined by a set of genes (parameters) that make up their DNA strand or chromosome. Each gene is made up of alleles (binary bits) that can be converted to a corresponding decimal form. The chromosome of the individual can then be tested for a fitness value via the computational method being used. Typically the fitness value is a value of strength such as gain, cost or size that can be minimized or maximized.

This fitness value is used to rate the individual in order to decide upon selection for the next population. A member that is not selected for the next generation is permanently removed from the population. The selected members are then mated with one another and a new set of individuals replace the parents. These new members can be exactly the same as the parents or can be mated by swapping the genetic code of the parents. The new members can also undergo a mutation of their genes. This mutation can allow both good and bad traits to appear. Mutation is used to keep a population from prematurely converging to a weak solution (local maxima).

2.2 Applications of Genetic Algorithms

Since its conception, genetic algorithms have enjoyed global use by many researchers and scientists in many different areas. Although computer scientists can take much of the credit for the development of GA, areas such as business, science, and engineering have put the GA to good use. Engineers, who historically have been obsessed with better and cheaper, find particular interest in the GA.

In electromagnetics, most all problems are of a non-differentiable type. Some type of numerical solution is required to calculate the important characteristics of the problem. When the optimization is a goal, these problems lend themselves very well to the use of genetic algorithms. Antenna design is an area of electromagnetics that has recently benefited from the use of GAs. Rahmat-Samii and Michielssen [6] have lately compiled a great deal of work on antenna design using genetic algorithms.

Array thinning and array synthesis are two areas where genetic algorithms have proven their usefulness [7,8]. In both of these cases, the GA has provided results that exceed previous attempts to improve the array designs. A very unique application of the GA was to create an antenna that provides a hemispherical pattern [9]. This *genetic antenna* was created by providing the GA with a series of connected wires and a ground plane. The GA created an unconventional design of wires that indeed did provide an isotropic pattern above the ground plane.

Chapter 3 Genetic Algorithms

This chapter presents an in-depth explanation of each element of the genetic algorithm. A tutorial and an example of the GA application to wire antennas is also included. Section 3.1 provides an overview of the GA. Section 3.2 describes the variables and terms used to setup the GA. The processes of selection, mating and mutating are described in Section 3.3. Recommendations for a robust and properly converging GA are presented in Section 3.4. A simple example is used as a tutorial in Section 3.5 and a specific example of a wire antenna optimization is presented in Section 3.6.

3.1 Genetic Algorithms

Genetic algorithms are global optimizers of objective functions. The GA will evolve a population of solutions towards a goal by stochastically searching out the best characteristics of individuals in a population and using them to create a 'superior' species. Interestingly enough, there is no general GA theory to prove population convergence to a global or even a local optimum [10].

Genetic algorithms reach an optimal solution by following the concepts and parameters set by Darwin [5]. GAs utilize known concepts such as chromosomes, genes, alleles, mating, and mutation. Many authors have covered the setup of GAs [9-13]. The flowchart shown in Figure 3.1 outlines this technique.

Generate an Initial Population

- *Randomly generated quantized genes (binary)*
- *Each gene contains the 'genetic code' of each individual*

- Evaluate Fitness (or Objective) Function, *f(x)*
  - *'quality' of individuals in the population*
  - *Use numerical solver (i.e. NEC, Wire) to calculate properties such as Directivity, Bandwidth, etc..*
- Select the best members of the population based on Fitness
  - *There are many methods to select the best members*
- Crossover or mate the individuals in the population
  - *This occurs with a probability* p_{cross} $(.6 < p_{cross} < .9)$
  - *Choose two members, swap their genetic codes to create two new members.*
- Mutate the individuals
  - *This occurs rarely with a probability* p_{mut} $(0.001 < p_{mut} < 0.01)$
  - *This allows changes in the population to not only slow the convergence rate, but to also allow unique members to appear.*
- Evaluate Fitness again
- If the population has converged to a 'superior' race, end the process, otherwise loop back and continue.

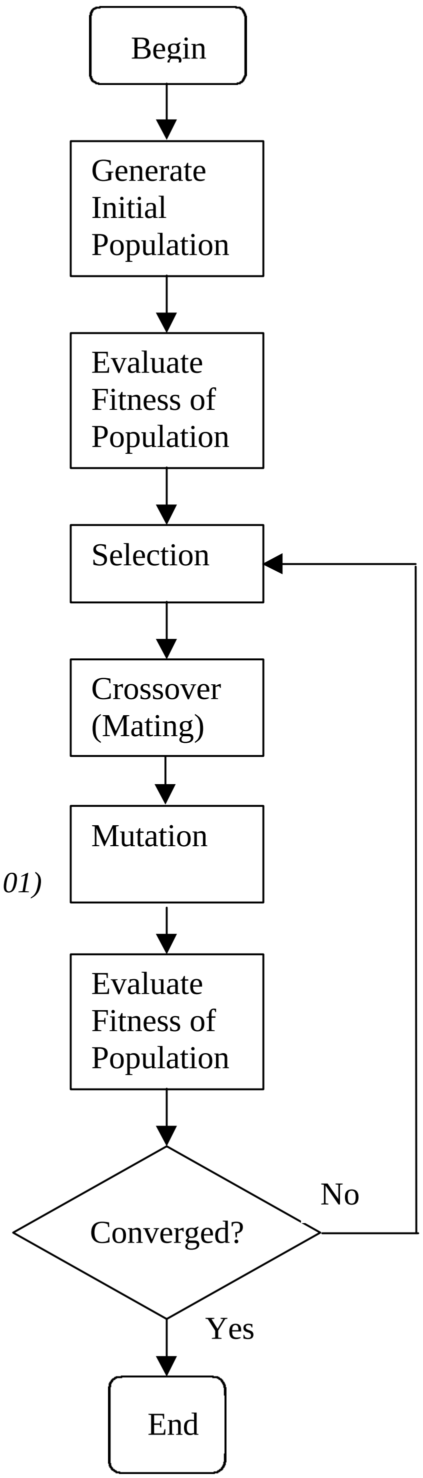

Figure 3.1: GA flowchart

3.2 GA Setup

Genetic algorithms attempt to optimize a fitness or objective function denoted as $f(\mathbf{p})$. A population of N individuals are tested using $f(\mathbf{p})$. Typically, $f(\mathbf{p})$ is some type of property determined by the numerical solver which provides the analysis of a specific design. In this particular project, the antenna code NEC2 [2] is used to calculate the properties of the antenna for the fitness function.

All of the parameters are assigned in Darwinian terms. The input, **p**, is the DNA strand or chromosome. This chromosome consists of a set of genes, denoted as,

$$\mathbf{p} = \{g_i \mid i = 1, 2, .. N_g\}, \tag{3.1}$$

where N_g is the number of genes that make up the chromosome. Each gene is considered a parameter of the problem. A gene is, in turn, made up of a string of alleles,

$$\mathbf{g} = \{a_i \mid i = 1, 2, .. N_a \}. \tag{3.2}$$

Typically, a binary alphabet {0,1} is used in order to discretize the parameters. The use of a binary alphabet simplifies operations such as mating and mutation. This is better visualized by the following example,

$$\mathbf{p} = \overbrace{a_1, a_2, ...a_{N1}}^{\mathbf{g}_1}\overbrace{a_{N1+1}, a_{N1+2}, ...a_{N2}}^{\mathbf{g}_2} \; ... \; \overbrace{a_{N(x-1)+1}, a_{N(x-1)+2}, ...a_{Nx}}^{\mathbf{g}_x}, \tag{3.3a}$$

$$\mathbf{p} = [\overbrace{10110111}^{g_1}\overbrace{11101000}^{g_2}...\overbrace{01101110}^{g_x}. \tag{3.3b}$$

In this example, a chromosome consists of *x* genes and each gene is of length 8. A gene is converted into decimal (base 10) form for use in *f*(**p**) using the following formula.

$$d_n = \sum_{i=1}^{N_a} g_n(i) \cdot 2^{M-i} \tag{3.4}$$

The decimal representation of the n^{th} gene includes a parameter M. This parameter controls where the decimal point lies. The value of M also affects the range of variables. For example, [1 1 1 1 1 1 1 1] with M = 10 yields 1020. The same bits with M = -10 yields 0.00097274. The number of discrete values attainable is 2^n.

The choice of gene length and M affect both the range of values and the number of discrete values that the gene can assume. For example, [0 0 0 0 0 0 0 1] with M = 10 yields 4. This allows the genes to take on discrete values that are ±4 units apart. On the other hand, when M = -10 the values are only ±3.8147e-6 units apart. Either value of M allows 2^8 or 256 discrete values. Once the binary genes are converted into decimal form, the fitness function *f*(p = $g_1,g_2,..g_{Nx}$) is readily evaluated.

3.3 GA Operations

Genetic algorithms exist in many different variations. An overview of the different options that currently exist for GAs is presented here. The different options affect the convergence rate of a GA. The convergence rate should be as quick as possible while allowing the GA to fully search for the global optimum.

3.3.1 Selection

Selection of individuals for the next population set is analogous to a lion taking down weak members of a herd of wildebeest. This survival-of-the-fittest cleansing allows for a healthier herd to emerge. Natural selection is an important process because the selection type affects the convergence rate of the population. Many of these selection schemes are covered by Johnson and Rahmat-Samii [12].

3.3.1.1 Population Decimation

Population decimation is the easiest method to implement. It requires the members of a population to be ranked (by fitness) from strongest to weakest. Members below a minimum ranking or fitness value are eliminated and the remaining members populate the next generation. This type of selection scheme is poor. Population decimation removes lower quality members of the population and too rapidly converges to an often-incorrect global maximum. Worthy characteristics, that some weaker members may contain, are prematurely removed. The loss of weaker members can occur long before the beneficial effects of a unique characteristic are recognized by the evolutionary process [12].

GAs possess great power in their ability to globally search for an optimum solution. A GA can quickly get on the wrong track when population diversity is prematurely reduced using population decimation. Once these unique characteristics are removed from the gene pool, the GA can reintroduce the lost characteristics by way of mutation. Reintroduction of a lost gene characteristic by mutation is improbable.

3.3.1.2 Roulette Wheel Selection

Roulette wheel selection (or tournament selection) uses the fitness value of each member to assign a probability of selection for the next generation. Equation (3.5) states the probability of selection. An identically sized population is created by randomly selecting members relative to their probability

$$p_{selection} = \frac{f(parent_i)}{\sum_i (parent_i)}. \tag{3.5}$$

Members with a low fitness value are selected less often than members with a high fitness value. This selection method not only allows stronger members to pass on, but also gives a fighting chance for weaker members, which may possess important characteristics, to survive and mate.

3.3.1.3 Tournament Selection

A more effective selection method is tournament selection. In tournament selection N members are chosen at random. From this group of N individuals the strongest members are selected. The process is repeated until the members for the next, identically sized, population are selected. Tournament selection allows both weaker and stronger members of the population to be selected. This method, compared to roulette wheel selection, converges slightly faster to a global maximum because the very weakest members are rarely selected.

3.3.2 Crossover

Mating, or crossover, is used to create the next generation. This process is done by randomly selecting two members from the population. A crossover point, k, is randomly selected and the two parents are mated with a probability of p_{cross}. If the two parents are not mated (with probability $p_{cross} – 1$), both members are simply placed into the next generation’s group. From parent 1, all of the genes preceding the crossover point are used for child 1. The genes following the crossover point from parent 2 are retrieved and used for child 1. Child 2 is created in a similar fashion. Figure 3.2 illustrates the crossover procedure.

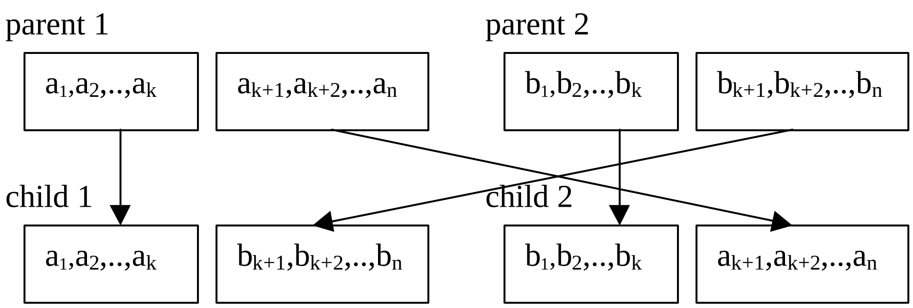

Figure 3.2 The crossover (mating) process is done by splitting the chromosomes of the parents at the crossover point, k, and swapping their genetic code (alleles).

More than one crossover point is possible. Multiple crossover points allow more complicated schemes for mating which may offer advantages to population diversity. A thorough study of the p_{cross} value would be beneficial. Currently, the range of 0.7 to 0.9 for p_{cross} is accepted. A large p_{cross} ensures a widespread search of different solutions, while a smaller p_{cross} converges faster. The effects of incest could also be studied in future investigations. Perhaps better use of the population is possible if members from differing family trees are used during mating.

3.3.3 Mutation

Just as in nature, mutation allows the population to change by introduction of random characteristics. Without mutation the population would quickly converge to a solution that may or may not be correct. Mutation is necessary for a population to continually evolve towards a 'superior' species. Mutation randomly chooses alleles to alter with a probability p_{mut}. This mutation usually results in poor fitness, but occasionally it increases the fitness value. This singular increase instance is important for the species. The probability of mutation is generally very small; $0.001 < p_{mut} < 0.01$ [10].

3.3.4 Elitist Strategy

Elitist strategy is utilized to guarantee monotonically increasing population fitness [12]. It is not uncommon for the best members of a population to be mutated, mated or selected out of existence. Elitist strategy keeps track of the best member of the group and ensures that the member's genes continue on to the next generation.

Elitist strategy copies the best member after the first evaluation of the population. Then, after selection, mating, mutating, and re-evaluation, the program tests to see if the best member of the new population is equal to or superior to the saved member. If it is not, the best member from the previous population is inserted into the new population.

3.4 Recommendations

Larger population sizes tend to converge to an optimum solution with fewer generations. This is because the solution space is sufficiently covered with a larger population size. This luxury may not be affordable if the fitness function is too time consuming. Also, it may be redundant to use such a thorough initial search space. A tradeoff occurs between population size and the time needed to converge to a solution. A small population converges quickly, but may not find a global optimum. A large population converges slowly, but more confidently finds the global optimum. Judicious choices of gene and population size are important, and dependent on the particular problem.

Gene length (number of alleles or bits) is set relative to how accurate an answer is needed. Larger gene length allows more quantization levels. It is also necessary to judiciously choose M from equation (3.4). The parameter M affects the range of values that the gene can assume. The gene length affects the accuracy of the solution and the variable M affects the size of the solution space.

It is generally accepted to choose a population size that is 2 to 3 times larger than the total chromosome length (total number of bits). For instance a chromosome with 4 genes (parameters) that each contain 10 alleles (bits) should have a population of 80 – 120. Larger populations require more simulations per generation, but in general require fewer generations to find a solution. This is merely because the initial search space is so large. This may not be necessary for simple problems. However, more complex problems, the majority of the initial population may be unacceptable and the next generation is filled with the very few members that survived the selection process. In fact, sometimes the initial population is filled with no acceptable solutions at all! This is remedied by allowing a larger initial population and thus a more thorough initial search.

Tournament selection should be used with selection groups of 3-10, relative to the population size. Elitist strategy is important in order to maintain a monotonically increasing species fitness. The probabilities of crossover and mutation should be set to $0.6 < p_{cross} < 0.9$ and $0.001 < p_{mut} < 0.01$.

The genetic algorithm itself does not converge down to the exact solution. It is very good at hunting down the approximate solution but does not achieve the perfect solution each time. This fact becomes obvious when multiple runs of the GA turns up many different answers which all lie very close to one another. Therefore the use of another search routine after the initial GA search may be necessary. To take advantage of the GA that is already being used, simply create a new initial population that varies by ~5% from the previous GA result and rerun the GA. This will force the GA to significantly reduce its search space.

There is no current theory that proves that the genetic algorithm is capable of achieving the correct solution 100% of the time. This is because the GA is dependent on the correct setup of the problem. For instance, if the GA converges quickly to a wrong answer the population size is too small. These user issues are difficult to quantify into an exact formula for the setup of the GA.

3.5 A Simple Example

This section covers a simple example of how the GA functions. A fitness function given as

$$f(x) = 10-(x-7)^2 \tag{3.6}$$

is considered for this example. Only one chromosome, x, which has one gene is used. A chromosome value of 7 is the solution to this problem.

3.5.1 Initial Population

It is necessary to first choose a gene length and decimal point control M. The GA provides a more accurate answer when a longer gene length is chosen. A gene length of eight is acceptable in this case. The use of M controls the range of the variable. A look at f(x) in equation (3.6) shows that it is necessary to have genes spanning from 0 to 14. Using equation (3.4) to convert [1 1 1 1 1 1 1 1] to decimal with M = 4 yields d = 15.9375 which is sufficient to cover the range of values. In an actual problem, reference to a fitness function with a known solution as in equation (3.6) will not be available. In such cases the range of values (search space) must be judiciously chosen.

The next step is to generate a random population. As previously discussed in section 3.5, it is best to choose a population that is 2 to 3 times as large as the chromosome length. A population of 10 is chosen to simplify the pictured tables. Each allele of the population is a randomly chosen value of 0 or 1. Figure 3.3 shows the initial population and their corresponding fitness function values for the problem. Evaluation of the fitness function in an actual multi-parameter problem is generally very time consuming and is always the limiting time constraint.

$$\underbrace{\begin{bmatrix} 1&0&0&0&0&1&0&0\\ 0&1&0&1&0&1&1&0\\ 1&1&0&1&0&1&0&0\\ 1&0&0&0&0&1&0&1\\ 1&0&1&1&1&1&1&1\\ 0&0&0&1&1&1&1&1\\ 0&0&1&1&0&1&0&1\\ 0&0&0&0&1&1&1&1\\ 1&0&0&0&0&1&0&0\\ 0&1&1&1&1&1&1&0 \end{bmatrix}}_{\text{initial population chromosomes}} \Rightarrow \underbrace{\begin{bmatrix} 8.2500\\ 5.3750\\ 13.2500\\ 8.3125\\ 11.9375\\ 1.9375\\ 3.3125\\ 0.9375\\ 8.2500\\ 7.8750 \end{bmatrix}}_{x = \text{decimal form}} \Rightarrow \underbrace{\begin{bmatrix} 8.4375\\ 7.3594\\ -29.0625\\ 8.2773\\ -14.3789\\ -15.6289\\ -3.5977\\ -26.7539\\ 8.4375\\ 9.2344 \end{bmatrix}}_{f(x)\ \text{fitness}}$$

Figure 3.3 Initial population converted to decimal and evaluated.

3.5.2 Elitist Strategy

It is best to select and store the best member of the population. When the selection, mating and mutating of the population is done, the fitness of the population is tested. If none of the members of the new generation are superior to the previous populations' elite member, then a randomly chosen member of the new generation is replaced with the elite member. This is done to force the population's fitness to monotonically increase.

In this example, the elite member is the member with the decimal chromosome value of 7.875 and the fitness value of 9.2344. This member will be stored until the selection, mating and mutating processes are finished.

3.5.3 Selection, Mating and Mutating

Tournament selection is chosen because of its fast convergence rate. A pool of *three* randomly chosen members is grouped and the best of the group is selected for the next population. The selection process is repeated until an equal size population is created. Figure 3.4 shows the selected population. Note that the majority of the members are closer to the solution, x = 7, than the previous population shown in Figure 3.3.

Next, the selected members are mated. Two members are removed from the selected group in Figure 3.4 at random and with a probability of $p_{cross} = 0.7$ they are mated. If the two selected members do not mate (30% chance), they are merely placed into the next population set. This process continues until all the members are assembled into the next population set.

$$
\underbrace{\begin{bmatrix}
1 & 0 & 0 & 0 & 0 & 1 & 0 & 1 \\
0 & 1 & 0 & 1 & 0 & 1 & 1 & 0 \\
0 & 0 & 1 & 1 & 0 & 1 & 0 & 1 \\
1 & 0 & 0 & 0 & 0 & 1 & 0 & 0 \\
1 & 0 & 0 & 0 & 0 & 1 & 0 & 0 \\
0 & 1 & 1 & 1 & 1 & 1 & 1 & 0 \\
1 & 0 & 0 & 0 & 0 & 1 & 0 & 0 \\
0 & 1 & 1 & 1 & 1 & 1 & 1 & 0 \\
0 & 1 & 0 & 1 & 0 & 1 & 1 & 0 \\
0 & 0 & 1 & 1 & 0 & 1 & 0 & 1
\end{bmatrix}}_{\text{selected members from the first population}} \Rightarrow \underbrace{\begin{bmatrix}
8.3125 \\ 5.3750 \\ 3.3125 \\ 8.2500 \\ 8.2500 \\ 7.8750 \\ 8.2500 \\ 7.8750 \\ 5.3750 \\ 3.3125
\end{bmatrix}}_{x = \text{decimal form}}
$$

Figure 3.4 The members selected using tournament selection.

To mate the selected members a crossover point is randomly chosen. In this case the crossover point is an integer between 0 and 7. The two chosen members swap their genetic code at the crossover point. Figure 3.5 illustrates this process.

$$
\begin{bmatrix}
1 & 0 & 0 & 0 & 0 & 1 & 0 & 1 \\
0 & 1 & 0 & 1 & 0 & 1 & 1 & 0
\end{bmatrix}
$$

The two selected members

Crossover point = 5

$$
\begin{bmatrix}
1 & 0 & 0 & 0 & 0 & 1 & 1 & 0 \\
0 & 1 & 0 & 1 & 0 & 1 & 0 & 1
\end{bmatrix}
$$

The two ‘children’ of the members

Figure 3.5 To illustrate the mating procedure.

Figure 3.6 displays the resulting population after the selection and mating processes has been implemented. The population has both good and bad members. One member, 7.3125, is clearly closer to the objective of value 7, but 1.375 is not. The next generation will most likely produce more members with x = 7.3 and less members with x = 1.3. Already the algorithm is rooting out solutions.

Mutation takes place after the selection and mating processes are complete. Mutation is used during the early generations to generate new and unique solutions. Mutation is used in later generations to keep the population from prematurely converging towards an incorrect solution.

$$\underbrace{\begin{bmatrix} 1 & 0 & 0 & 0 & 0 & 1 & 1 & 0 \\ 0 & 1 & 0 & 1 & 0 & 1 & 0 & 1 \\ 0 & 0 & 1 & 1 & 0 & 1 & 0 & 1 \\ 1 & 0 & 0 & 0 & 0 & 1 & 0 & 0 \\ 1 & 0 & 0 & 1 & 1 & 1 & 1 & 0 \\ 0 & 1 & 1 & 0 & 0 & 1 & 0 & 0 \\ 1 & 0 & 0 & 0 & 0 & 1 & 0 & 0 \\ 0 & 1 & 1 & 1 & 1 & 1 & 1 & 0 \\ 0 & 1 & 1 & 1 & 0 & 1 & 0 & 1 \\ 0 & 0 & 0 & 1 & 0 & 1 & 1 & 0 \end{bmatrix}}_{\text{mated group}} \Rightarrow \underbrace{\begin{bmatrix} 8.3750 \\ 5.3125 \\ 3.3125 \\ 8.2500 \\ 9.8750 \\ 6.2500 \\ 8.2500 \\ 7.8750 \\ 7.3125 \\ 1.3750 \end{bmatrix}}_{x\text{ =decimal form}}$$

Figure 3.6 The mated population.

A mutation probability (p_{mut}) of 0.01 is used in this example. Figure 3.7 shows the mutated group. One of the mutated alleles produced a good result, x = 7.3, and the other mutated allele generated a bad result, x = 0.25.

Mutated alleles

$$\underbrace{\begin{bmatrix} 1 & 0 & 0 & 0 & 0 & 1 & 1 & 0 \\ 0 & 1 & 0 & 1 & 0 & 1 & 0 & 1 \\ 0 & 1 & 1 & 1 & 0 & 1 & 0 & 1 \\ 1 & 0 & 0 & 0 & 0 & 1 & 0 & 0 \\ 1 & 0 & 0 & 1 & 1 & 1 & 1 & 0 \\ 0 & 1 & 1 & 0 & 0 & 1 & 0 & 0 \\ 0 & 0 & 0 & 0 & 0 & 1 & 0 & 0 \\ 0 & 1 & 1 & 1 & 1 & 1 & 1 & 0 \\ 0 & 1 & 1 & 1 & 0 & 1 & 0 & 1 \\ 0 & 0 & 0 & 1 & 0 & 1 & 1 & 0 \end{bmatrix}}_{\text{mutated group}} \Rightarrow \underbrace{\begin{bmatrix} 8.3750 \\ 5.3125 \\ 7.3125 \\ 8.2500 \\ 9.8750 \\ 6.2500 \\ 0.2500 \\ 7.8750 \\ 7.3125 \\ 1.3750 \end{bmatrix}}_{x=\text{decimal form}}$$

Resulting decimal form

Figure 3.7: Mutated population.

Figure 3.8 displays the final result of the selection, mating and mutating. This generation is healthier than the initial population and the elite member from the last generation is not needed. Therefore, we choose the best member from this population as our new elite member.

$$\underbrace{\begin{bmatrix} 1 & 0 & 0 & 0 & 0 & 1 & 1 & 0 \\ 0 & 1 & 0 & 1 & 0 & 1 & 0 & 1 \\ 0 & 1 & 1 & 1 & 0 & 1 & 0 & 1 \\ 1 & 0 & 0 & 0 & 0 & 1 & 0 & 0 \\ 1 & 0 & 0 & 1 & 1 & 1 & 1 & 0 \\ 0 & 1 & 1 & 0 & 0 & 1 & 0 & 0 \\ 0 & 0 & 0 & 0 & 0 & 1 & 0 & 0 \\ 0 & 1 & 1 & 1 & 1 & 1 & 1 & 0 \\ 0 & 1 & 1 & 1 & 0 & 1 & 0 & 1 \\ 0 & 0 & 0 & 1 & 0 & 1 & 1 & 0 \end{bmatrix}}_{\text{next generation}} \Rightarrow \underbrace{\begin{bmatrix} 8.3750 \\ 5.3125 \\ 7.3125 \\ 8.2500 \\ 9.8750 \\ 6.2500 \\ 0.2500 \\ 7.8750 \\ 7.3125 \\ 1.3750 \end{bmatrix}}_{x=\text{decimal form}} \Rightarrow \underbrace{\begin{bmatrix} 8.1094 \\ 7.1523 \\ 9.9023 \\ 8.4375 \\ 1.7344 \\ 9.4375 \\ -35.5625 \\ 9.2344 \\ 9.9023 \\ -21.6406 \end{bmatrix}}_{\text{fitness tested}}$$

Optimum members

Figure 3.8: The population that will serve as the next generation.

The GA now tests to see if the group has converged to one solution. If is has not converged it continues selecting, mating and mutating until the population converges to a single solution (see Figure 3.1). Convergence usually requires between 6 and 20 generations. This example took 7 generations before converging to [0 1 1 1 0 0 0 0] or 7, which is the exact solution to $f(x) = 10 - (x - 7)^2$.

3.6 Application to Antenna Problems, The Double Vee-Dipole

The following is an example of how to correctly setup and complete a GA antenna design. It is presented as a proof of the GA's effectiveness. This example reduces a brute force method of approximately 500,000 simulations to a mere 13,500 simulations!

It is well known that taking a standard dipole and bending it into a vee-dipole results in a higher directivity [14,15]. Safaai-Jazi recently hypothesized that adding two more arms will further increase the directivity, and Patwari investigated these ideas. The results of their investigations are presented in [3]. The geometry of this double-vee dipole is illustrated in Figure 3.9.

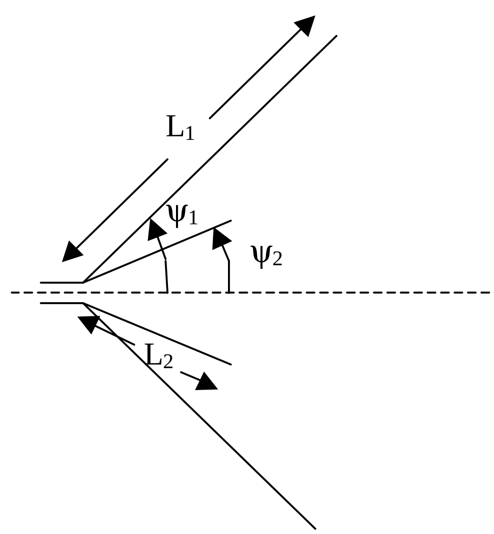

Figure 3.9 Double vee-dipole geometry and parameters.

This antenna was selected for a GA study because it presents a significant challenge for a brute force study. This antenna lends itself well for use in a GA optimizer because it has a set geometry with obvious variable limits on angles and lengths of the antenna arms. This study attempts to repeat the work done by Patwari and Safaai-Jazi and achieve essentially the same results with far fewer simulations.

3.6.1 Setup

This particular design requires three independent variables. The larger arm length, L_1, is kept to a known value and the directivity is maximized by varying the smaller arm length, L_2, and the angles ψ_1 and ψ_2. In this study, the genes (L_2, ψ_1, ψ_2) have 8 alleles (bits) each. Therefore, each chromosome is 24 bits long. A population of $3\times24 = 72$ is used. This means that each generation must undergo 72 simulations. Figure 3.10 is an example of the chromosome structure and its decimal equivalent. Use equation (3.4) to convert the binary gene to decimal. M = 2 is used for the length L_1 and M = 6 is used for the angles. With M = 6 for the angles, a maximum angle of 63.75° is achievable with angle increments of 0.25°. For M = 2 for the length L_1, a maximum length of 3.98m is achieved with length increments of 0.0156m.

$$\underbrace{\left[\underbrace{0\,0\,1\,0\,1\,1\,0\,1}_{L_2 \text{ gene} = 0.703l}\ \underbrace{1\,1\,0\,1\,0\,1\,0\,1}_{y_2 \text{ gene} = 53.25^\circ}\ \underbrace{0\,1\,0\,1\,1\,1\,1\,1}_{y_2 \text{ gene} = 23.75^\circ}\right]}_{\textit{chromosome}}$$

Figure 3.10 Example of a chromosome for the double vee-dipole.

For this study a p_{mut} of 0.01 and a p_{cross} of 0.7 are used. In addition to the standard procedures to choose probabilities and population sizes, there are other restrictions to keep in mind. The length, L_2, is required to be smaller than L_1 (otherwise it would simply extend indefinitely to increase directivity). Also, ψ_2 is required to be smaller than ψ_1 which in turn is limited to less than or equal to 63.75°. Another requirement is that the difference between ψ_1 and ψ_2 must be no smaller than 1 degree. This is a requirement of the NEC2 software.

The above restrictions are important, but could prove disastrous. ψ_2 is chosen to be smaller than ψ_1 because the footprint of the double-vee dipole is desired not to exceed that of a conventional vee dipole of arm length L_1. This knowledge greatly reduces the search space and thus the GA optimization time.

3.6.2 Solutions

The GA was run on a set of L_1's retrieved from N. Patwari's report. The program was estimated to need 500,000 NEC2 simulations to generate the solution set when using a brute-force search method. The GA found the solution set in only 13,636 simulation runs! The GA needed 16.4 hours to find the answers. It took over 600 hours (25 days) for the brute force method to run! All simulations were run on a Sparc Workstation with a 300MHz Pentium processor and 386 Megs of RAM.

Inspection of Figure 3.11 provides a graphical proof for the validity and effectiveness of the GA. The GA found all the peak solutions. In fact, because it's search routine is truly global over the provided search space, it found solutions that were had not been obtained. This example of GAs use on antenna problems shows the true power behind GAs. They can be used to intuitively converge towards solutions considerably faster than brute force methods.

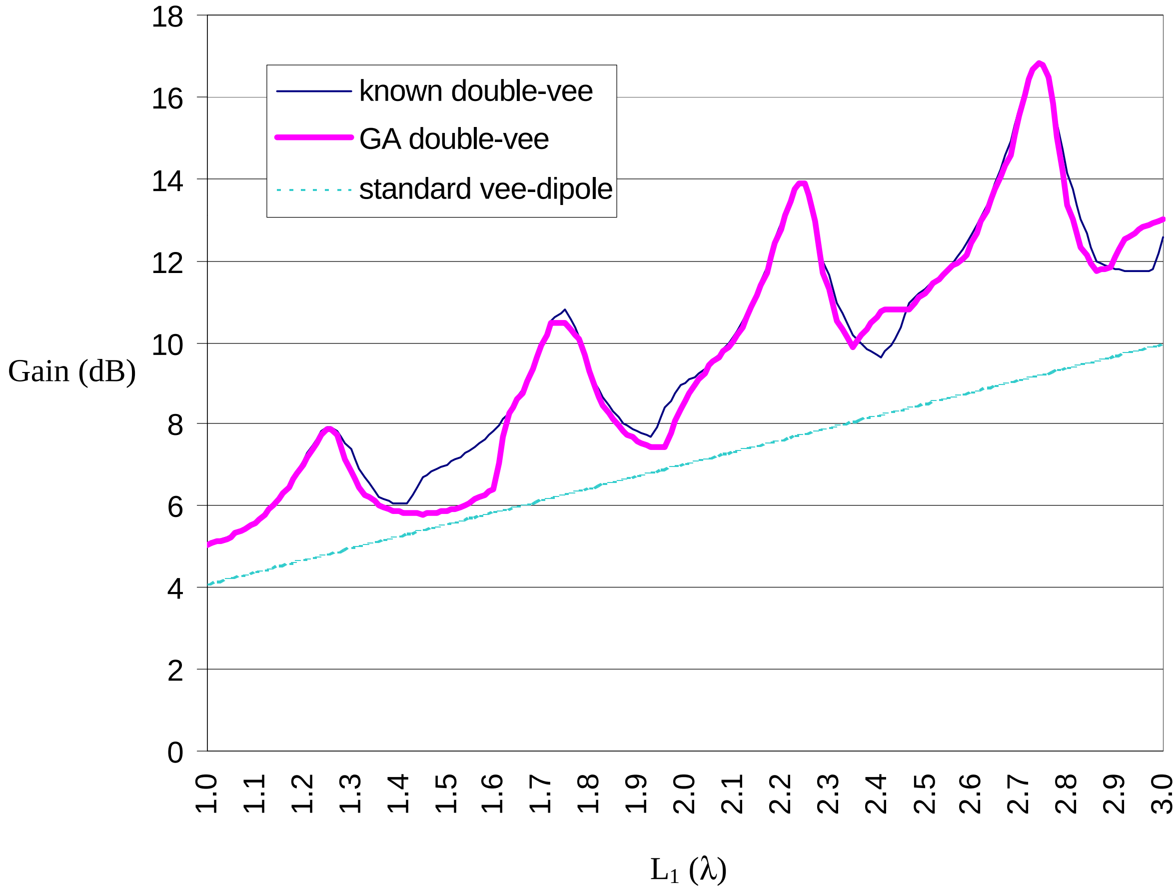

Figure 3.11 Comparison of known double vee-dipole with the GA double vee-dipole.

The program required an average of 164.3 NEC2 simulations for the GA to converge to a solution. Using a workstation it took an average of 11.83 minutes to find a solution for any particular length of L_1. An average of 9.4 generations was needed to converge to a solution. The simulations took longer to run with increasing L_1 length. This is merely because of the numerical solver (NEC2) having to solve a larger structure.

Chapter 4 The Helical Antenna

This chapter reviews the basic helical antenna and its variations that improve gain, axial-ratio and bandwidth. This review will facilitate the comparison of the conventional helix to the optimized helix that is created by the genetic algorithm as discussed in chapter five.

Section 4.1 covers the basic operational theory of the conventional helix. Section 4.2 reviews many of the variations on the conventional helix. These variations attempt to provide better gain, bandwidth, and/or axial-ratio performance. Section 4.3 presents NEC2 simulation results of a conventional helix. These results are compared to known results of the conventional helix available in the literature, therefore ascertaining the accuracy of NEC2.

4.1 Conventional Helical Antenna

The purpose of this section is to provide a basic understanding of the helix in order to gain insight for setting up the genetic algorithm properly. The helix was chosen for this study because of its distinct parameters and defined shape. Also, because a rigorous solution to the helix does not exist [16], a numerical solver (NEC2) must be used in order to find the radiation properties of a given helix configuration. The use of a numerical solver does not provide any insight as to how an optimal helix configuration may be obtained. This optimal helix configuration must be rooted out by an optimization scheme such as the genetic algorithm.

The main distinction of the helix over other wire antennas is its ability to produce a circularly polarized (CP) wave. This CP wave is produced when the helix is operating in the axial-mode regime. The axial mode occurs when the charge distribution along the helix is such that the phase changes by 180° over a half turn. This phase change produces far fields that interfere destructively with one another in directions normal to the axis of the helix. This also produces far fields that interfere constructively along the axis of the helix. This constructive interference, along with a ground plane that provides a strong image (as in the case of a monopole above a ground plane), produces a relatively directive beam traveling out of the top of the helical structure.

The helical antenna is considered a traveling-wave antenna if the path of the wire that makes up the antenna is long enough, ($L > \lambda/2$) [16]. The current traveling along the length of wire is heavily attenuated by the time it reaches the top of the structure. This in turn produces a relatively small reflected wave from the open end of the structure. This effect provides a low VSWR and relatively constant input impedance across a wide bandwidth [17].

In order for the helix to operate in the axial mode, certain parameter specifications originally defined by Kraus [18] must be met. The following parameters are used to define the geometry of the helix.

D = diameter of helix (center to center)
C = circumference of helix = πD
S = spacing between turns (center to center) = $C \tan \alpha$
α = pitch angle = $\tan^{-1}(S/C)$
ℓ = length of one turn = $(C^2 + S^2)^{1/2}$
N = number of turns
L = length of helix coil = $N\ell$
h = height = axial length = NS
d = diameter of helix conductor

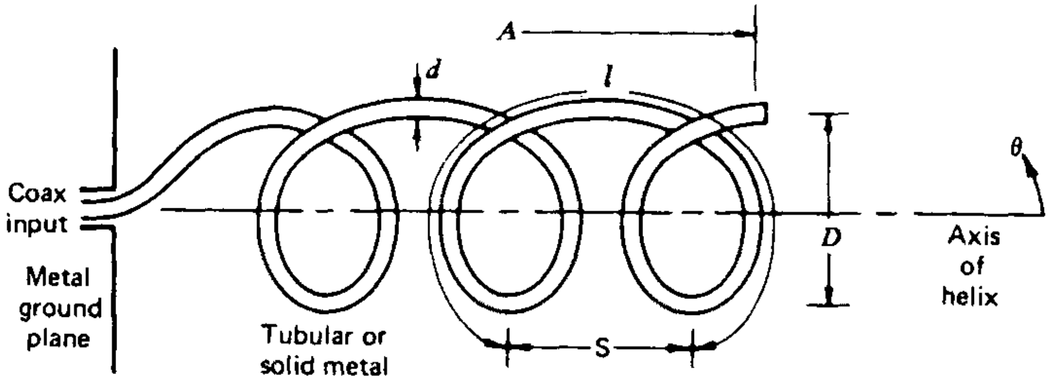

Figure 4.1 Conventional helix antenna geometry.

A conventional helix operates in the axial mode when the circumference is on the order of one wavelength. This circumference allows a 180° phase shift over a half turn as discussed earlier. A very rough estimate of the bandwidth can be obtained from the following relationship between wavelength and circumference [15].

This provides a bandwidth ratio of

$$\frac{f_u}{f_l} = \frac{c/l_u}{c/l_l} = \frac{4/3}{3/4} = 1.78 \qquad (4.2)$$

In practical situations, this bandwidth ratio estimate of 1.78:1 turns out to be quite optimistic. A more realistic bandwidth ratio is about 1.5. In general, the bandwidth decreases when the number of turns is increased. Therefore, (4.2) exists as an upper limit of the bandwidth of the conventional helix. A more accurate bandwidth ratio has been obtained empirically by King and Wong [19] for helical antennas with turns from 5 to 35.

$$\frac{f_h}{f_l} \approx 1.07\left(\frac{0.91}{G \big/ G_p}\right)^{4 \big/ 3\sqrt{N}} = 1.07\left(\frac{0.91}{10^{-3/10}}\right)^{4 \big/ 3\sqrt{N}}. \qquad (4.3)$$

Equation (4.3) is expressed in terms of the number of turns (N) and is formulated based on gain over peak gain equal to –3dB. These results generally agree with the work done by Maclean and Kouyoumjian [20]. From Figure 4.2 it is clear that the highest attainable bandwidth ratio is still below the predicted 1.78 from (4.2). Notice that the bandwidth ratio reaches a limit as N increases.

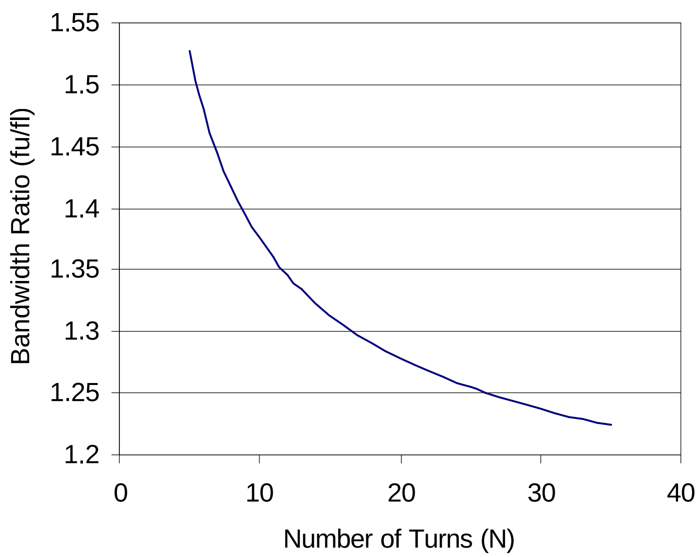

Figure 4.2 Bandwidth ratio versus number of turns from equation (4.3).

The empirical relation for the gain of a conventional helix can be expressed as [19]

$$G_p = 8.3\left(\frac{pD}{l_p}\right)^{\sqrt{N+2}-1}\left(\frac{NS}{l_p}\right)^{0.8}\left[\frac{\tan 12.5^\circ}{\tan a}\right]^{\sqrt{N}/2}. \qquad (4.4)$$

In (4.4), λ_p is the wavelength corresponding to the peak gain. Notice that the peak gain increases non-linearly with the number of turns (N). Figure 4.3 shows the relationship between peak gain and number of turns. Figure 4.4 displays the typical gain plots of various length conventional helix with a constant pitch angle.

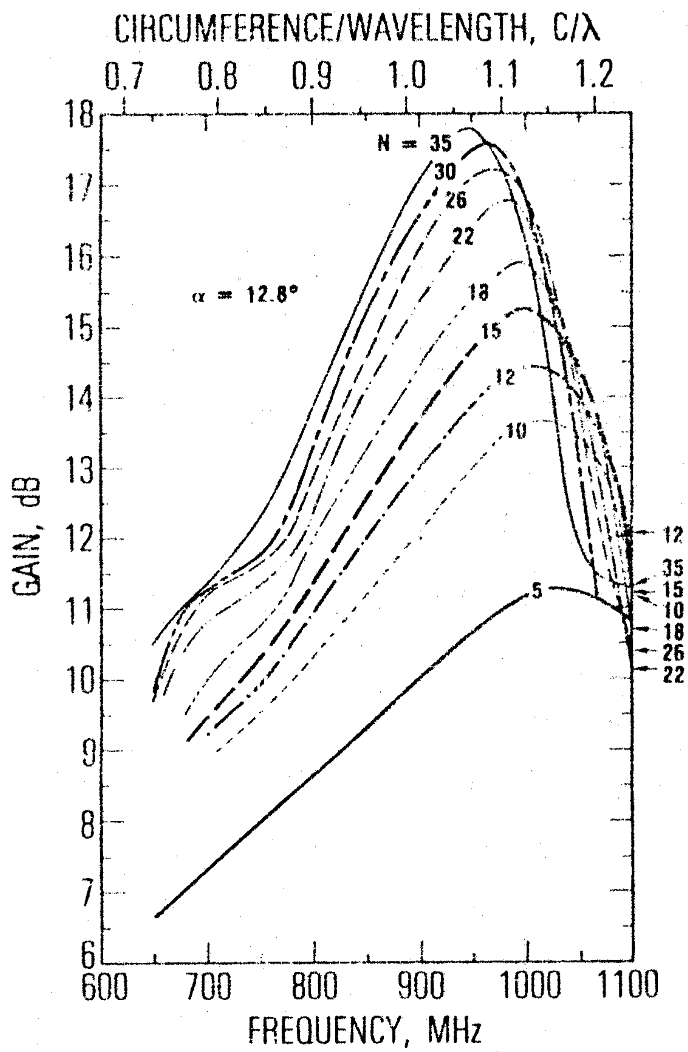

Figure 4.4 Gain versus frequency for a 5- to 35-turn helix; α = 12.8°, D = 107.4mm [19].

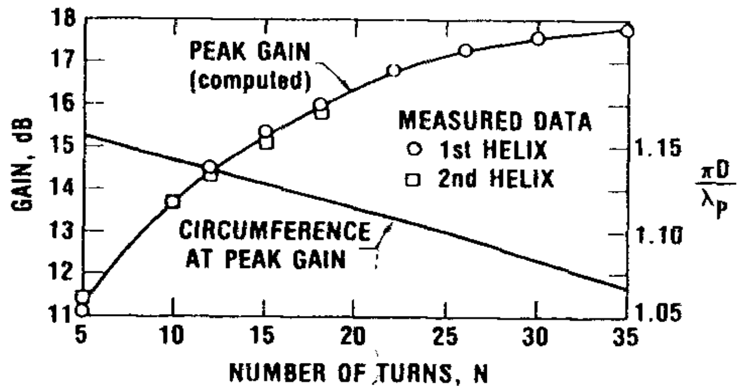

Figure 4.3 Peak gain of a variable-length helix with the pitch angle (α) = 12.8° [19].

Axial-ratio is another important characteristic to consider. A crude approximation for the axial-ratio is [15]

$$|AR| = \frac{2N+1}{2N}. \qquad (4.5)$$

This indicates that as the number of turns increase the axial ratio improves. Equation (4.6) is approximate at best and may be used to show the trend of the axial ratio with respect to number of turns.

The input impedance of the axial-mode helix is nearly purely resistive and relatively insensitive to changes in frequency. An empirical relation for the radiation resistance is [18]

$$R = 140\frac{C}{l}\ \Omega \qquad (4.6)$$

This expression is approximate and should be accurate to within a range of ± 20%.

It is now possible to observe the fundamental design tradeoffs for the conventional helix. As the number of turns increase, the gain increases and the axial ratio improves while the bandwidth decreases. Also, a larger number of turns implies a larger size antenna. The tradeoff between gain and bandwidth versus the tradeoff between gain and size are important to observe when designing a helix.

The parameters used to define the path of the helix must be properly set in order to achieve a desirable performance. Table 4.1 summarizes the ranges of different parameters.

Table 4.1 Parameter limits for conventional helix.

Parameter	Range
circumference (C)	$0.75\lambda < C < 1.25\lambda$
pitch angle (α)	$11° < \alpha < 14°$
number of turns (N)	$3 < N < 20$
diameter of ground plane	at least 0.5λ

These limits are a general guide provided by the many studies done on conventional helices [18-20]. The circumference that provides a peak gain at the design frequency is approximately 1.1λ [18]. Also, the optimal pitch angle that provides the highest gain is about 12.5°.

4.2 Modified Helical Antennas

In order to improve the performance of the conventional helix many modifications such as non-uniform diameter and tapering are used. These types of helices generally improve the bandwidth and increase the axial-ratio performance. Other designs attempt to reduce the size of the helix. All of the helix variations serve to improve the following performance values:

- Higher gain
- Larger bandwidth
- Lower axial-ratio
- Lower sidelobe level
- Lower VSWR at the feed
- Smaller size

In order to achieve these performance improvements countless helix variations have been suggested. Kraus has suggested three ways to modify the conventional helix [18]. Figure 4.5 shows these modifications and their various shapes.

- α constant, S and D variable
- D constant, α and S variable
- S constant, α and D variable

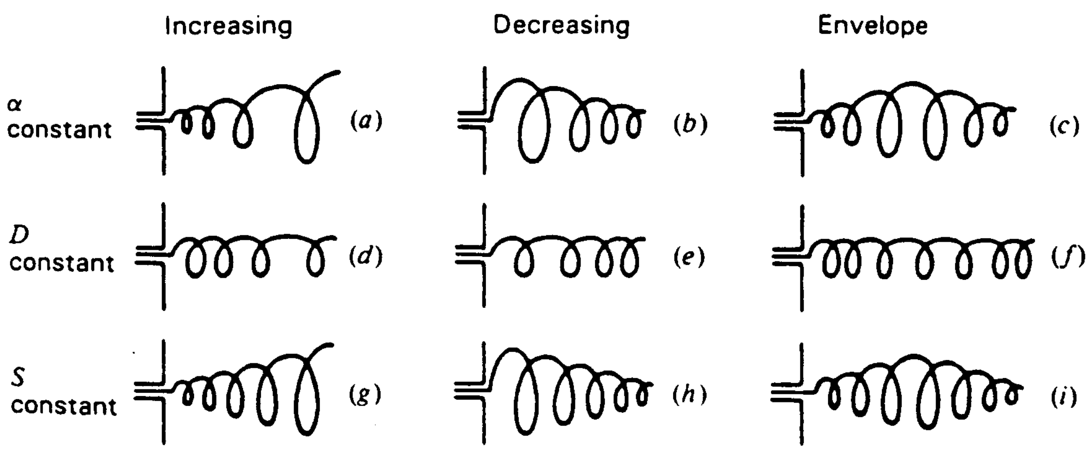

Figure 4.5 Variations of winding and tapering for the helix antenna [18]. (a) α constant while s and D vary. (b) D constant while α and s vary. (c) s constant while α and D vary.

Cupped ground planes are used to increase the gain and lower the sidelobe level. An axial-mode helix in a conical horn produces a significantly larger gain and lowers the sidelobe level [21]. These types of modifications do not attempt to change the helix itself; they merely attempt to narrow the beam produced by the helix.

Altering the conventional helix in discrete sections presents a simpler design than the continuous shapes suggested by Kraus. Figure 4.3 displays some designs developed and used to increase the bandwidth and lower the axial ratio. For instance, in order to decrease the axial ratio and the VSWR at the feed, the last few turns of the helix are tapered [22,23]. The reduction in the VSWR is achieved by suppression of the reflected currents by the tapered section.

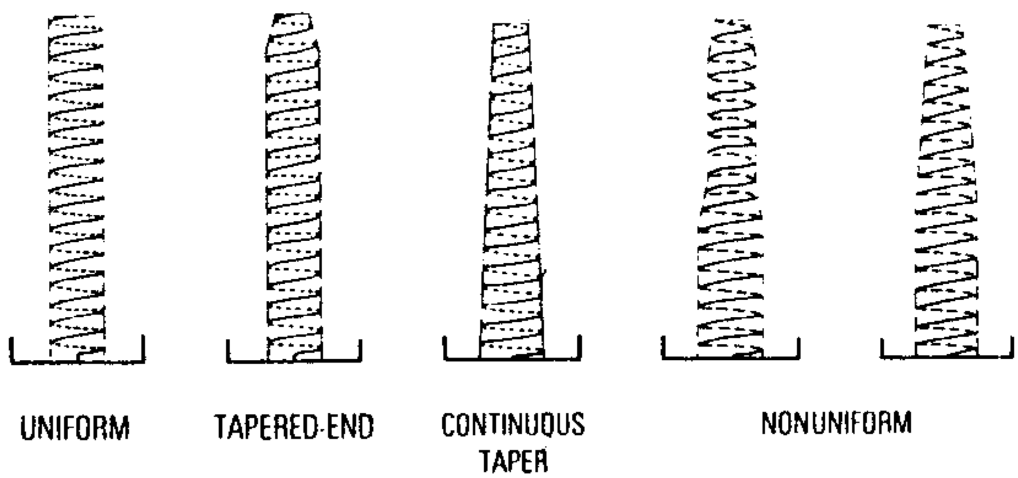

Figure 4.6 Various axial-mode helical antenna configurations.

A continuously tapered (see Figure 4.6c) helix tends to provide a larger bandwidth and lower the axial-ratio with a slight penalty in peak gain over the conventional helix [23]. A unique approach to further increasing the bandwidth while maintaining or increasing the gain is the nonuniform-diameter helix [24]. This type of helix uses two or more uniform helix sections of different diameters pieced together with tapered sections. The differing helix sections allow a larger bandwidth, lower axial-ratio and higher gain than the conventional helix. Figure 4.7 displays the gain and axial-ratio characteristics for two nonuniform-diameter helix designs. It is apparent from these graphs that the gain does not drop off as rapidly as a conventional helix in the upper frequency region.

Other modified helix shapes attempt to reduce the overall volume of the helix. The spherical helix wraps a wire around a spherical shape instead of a cylinder [25]. This design provides circular polarization over a wide beamwidth. A stub-loaded helix periodically places loading stubs around the circumference of each turn on a helix [26]. The stubs allow a longer electrical length (L) than the conventional helix. This allows the stub-loaded helix to provide similar performance to the conventional helix with a significant reduction in size.

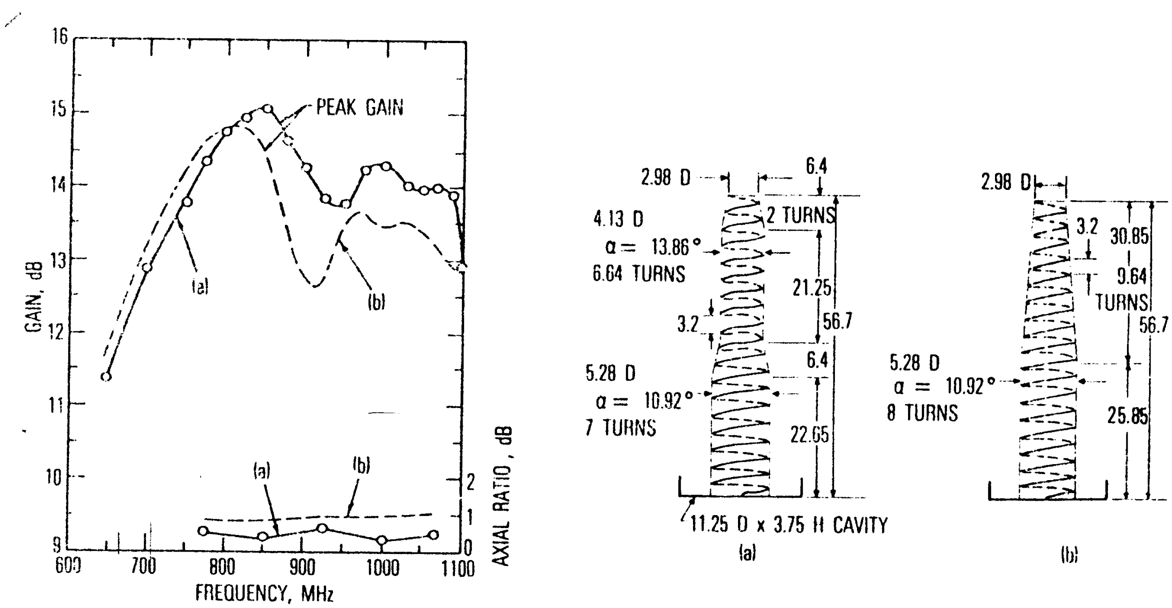

Figure 4.7 Gain and axial-ratio characteristics of two 17.64 turn nonuniform-diameter helices [22].

4.3 NEC2 Analysis of Axial-Mode Helix

The Numerical Electromagnetics Code (NEC, version 2) is a public domain moment-method code used to calculate radiation properties of wire structures [27]. In the case of a helix, NEC2 is used to apply a voltage source to the wire structure and compute far field patterns, input impedance and axial-ratio data. Calculation of the radiation properties of wire structures is based on numerical solutions of integral equations for currents induced by voltage sources [2].

Moment method codes break down large wire structures into many small segments for network analysis. Larger numbers of segments provide more accurate solutions and require longer computation times. This tradeoff is important to recognize because the NEC2 code performs as the fitness function for the genetic algorithm. If the choice of segmentation is unnecessarily large, a considerable amount of time is wasted in the fitness testing phase of the GA.

The curved wire that makes up the helical antenna is broken into a discrete number of straight segments per turn. Typically, each segment is required to be less that 0.1λ long. Testing was done to discover the optimal number of segments per turn by varying the number of segments and keeping track of directivity. Once the directivity settled into its correct value the number of segments per turn was recorded. The number of segments per turns used is 25. Thus, each segment is approximately $1/25^{th}$ of a wavelength or $0.04\lambda_d$, which is well below the required $0.1\lambda_d$ length.

The helical wire structure must be modeled above a ground plane. NEC2 provides a perfectly conducting infinite ground plane that allows very fast computation of the radiation fields in the forward directions ($-90° < \theta < 90°$). Surface patches as well as wire grids can be used to model finite ground planes. These finite ground planes allow radiation fields to be calculated in all directions ($-180° < \theta < 180°$). The drawback to using the finite ground planes is the time consumption. For instance, to calculate the radiation properties of a helix above an infinite ground plane it takes 6.76 seconds on a Pentium 450 MHz processor. To do the same calculation above a set of surface patches that model a finite ground plane takes 441.6 seconds! Therefore, a GA optimization run that requires 10,000 NEC2 runs would need 51 days using a finite ground plane versus 19 hours using an infinite ground plane. The time constraint is clearly unacceptable in this case. Also, information such as gain, input impedance, and axial ratio do not require back lobe data. Therefore the infinite ground plane is chosen for use in NEC2.

According to NEC2 documentation [27], angle between two intersecting segments must be large enough to prevent overlap between the two wires. The current distribution near the intersection is not reliable when overlap occurs. The same requirement applies when positioning the helical antenna above the ground plane. The helical antenna is modeled by placing the antenna $0.05\lambda_d$ above the ground plane and placing a segment between the bottom of the antenna and the ground plane (the antenna is not electrically attached to the ground plane). A voltage source is applied at the midpoint of this segment.

A great deal of work on axial-mode helical antennas has been done for modeling the helix in NEC2 [28]. The present work is done in order to reconcile the differences between Kraus, King and Wong, and Lee and Wong’s work on the conventional helix. While all three groups did work to discover empirical gain equations for the conventional helix, their results vary from group to group by as much as 5dB or 25%. Figure 4.8 compares the gain results from the three groups as well as from [28].

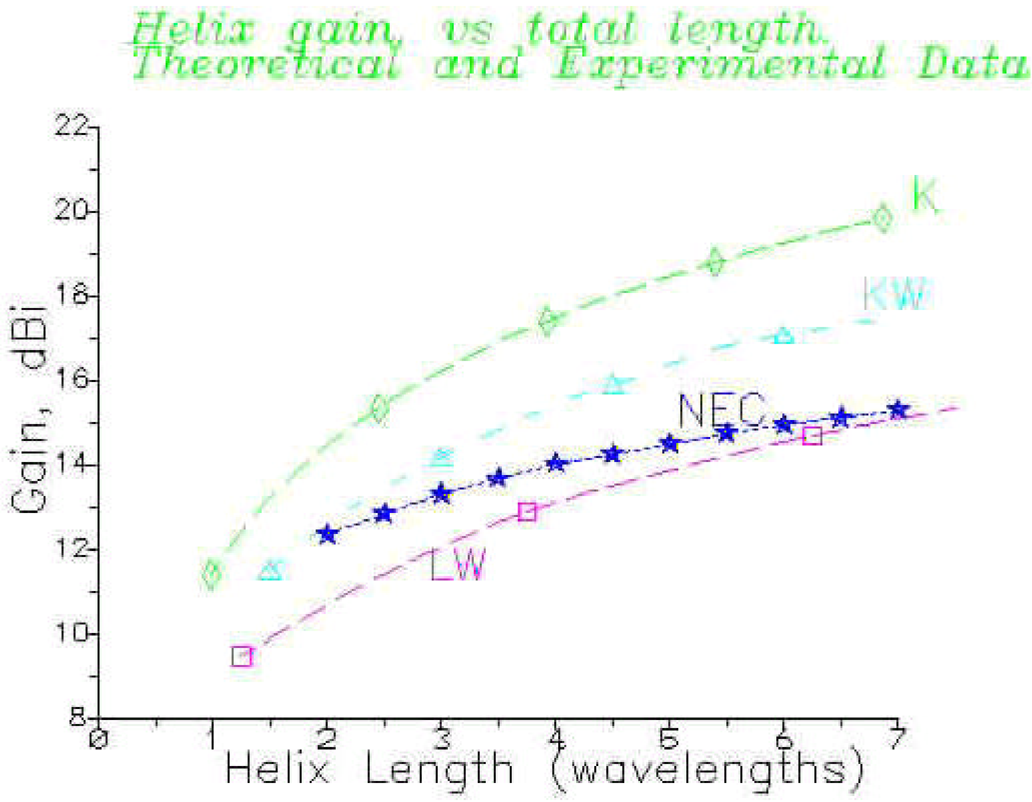

Figure 4.8 The peak gain of a helix as a function of length. K is the gain from the Kraus formula. KW is the gain from the measurements of King and Wong. LW is from the theory of Lee and Wong. NEC is from the numerical modeling of NEC2.

It is apparent from Figure 4.5 that Kraus's formula for gain is the most optimistic. The peak gain increases more slowly with respect to the antenna length than the Kraus' formula predicts. The King and Wong measurements were done using a small cavity that predictably increased the gain slightly [19]. The NEC2 results appear to be a compromise between King and Wong's work and Lee and Wong's work.

An empirical expression for peak gain is presented in [28] and is shown here as a comparison to Equation (4.4).

$$G_{\max}(dB) = 10.25 + 1.22h - 0.0726h^2 \tag{4.7}$$

Also presented is the radius at which the peak gain is possible. Both (4.7) and (4.8) are valid for heights (h) between 2 and 7 wavelengths.

$$R_{max} = 0.2025 - 0.0079h + 0.000515h^2 \qquad (4.8)$$

Figure 4.9 displays the gain versus the radius for different helix lengths (heights) from [14]. Equations (4.7) and (4.8) were empirically derived from Figure 4.9. The spacing between turns (S) is constant at 0.24λ for the helices in Figure 4.9. This figure is presented for use as a comparison to the model used in the project. Figure 4.10 illustrates the gain versus radius for different heights from the NEC2 model set up for use in this thesis. Note that Figure 4.9 matches Figure 4.10 very closely. This work is presented as a proof of the proper setup of NEC2 in order to trust the results given in future genetic algorithm optimization of the helix.

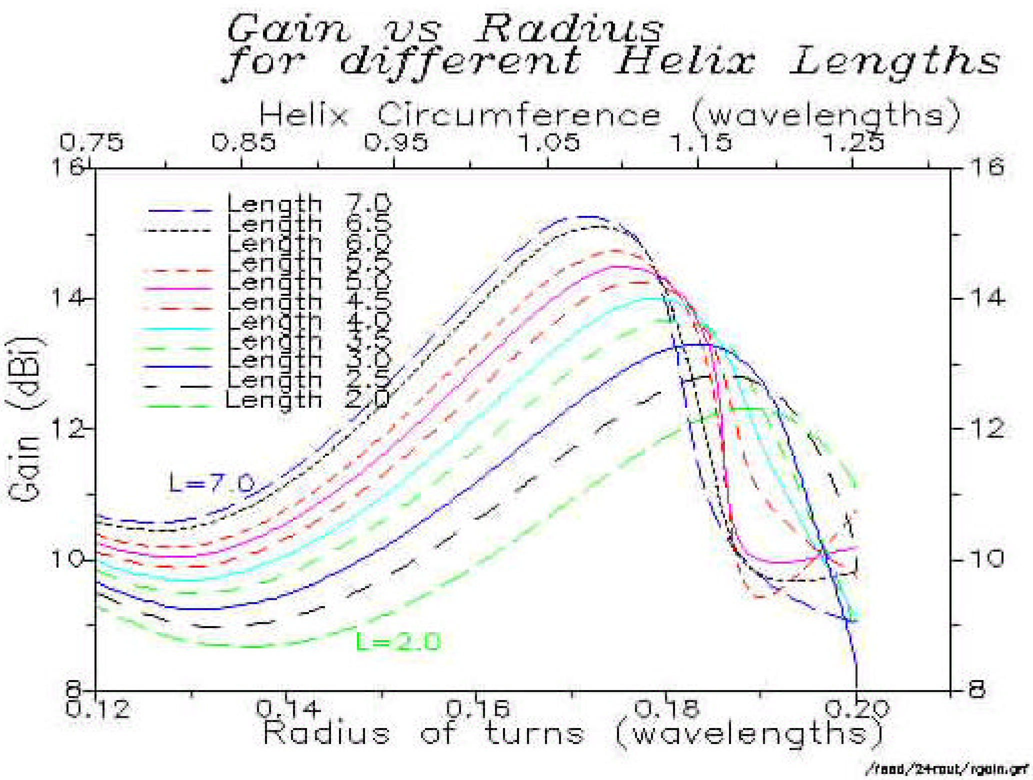

Figure 4.9 Plot of gain versus radius for several length helices. The spacing between turns in constant at 0.24λ. This plot is from the work done in [14].

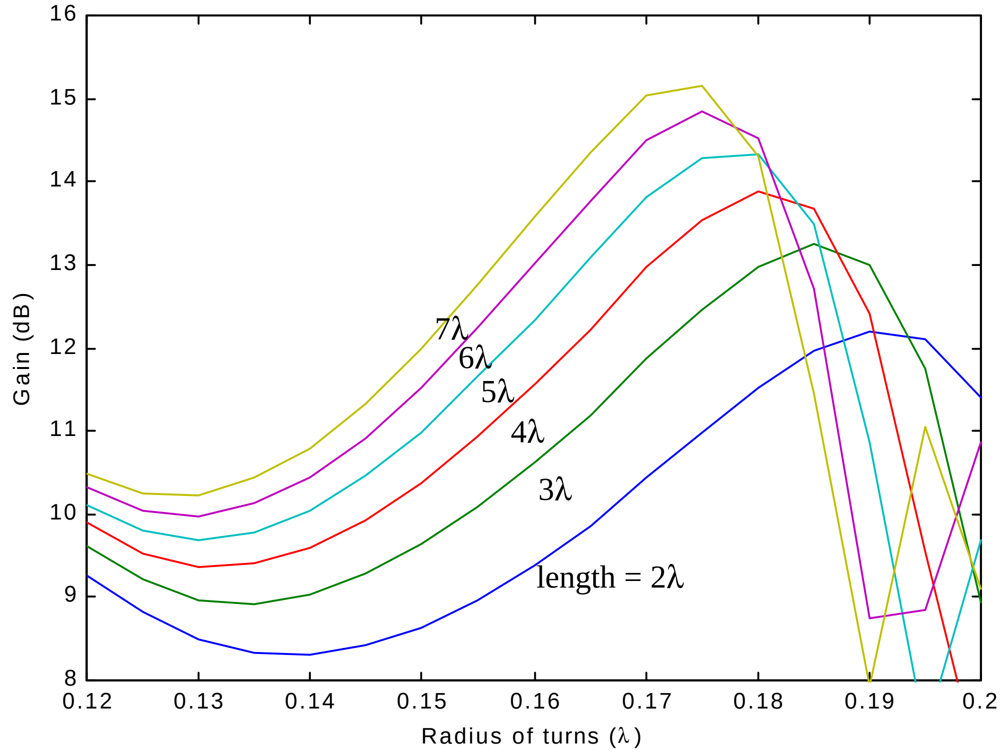

Figure 4.10 Plot of gain versus radius for several lengths of helices. The spacing between turns is constant at 0.24λ. This plot is from the NEC2 model used in this project.

Chapter 5 GA-Optimized Helix

In this chapter a GA is setup to discover a new design called the GA-optimized helix. This new design presented improves the bandwidth, axial-ratio, input impedance, and gain over the conventional helix. Section 5.2 overviews the basic shapes that the envelope containing the helix can assume. Section 5.3 explains how the fitness function is setup. The fitness function used here is unique, because this antenna requires the bandwidth, axial-ratio and gain to all be optimized. The setup and results are presented in sections 5.5 and 5.6. The GA-optimized helix is compared to the conventional helix in section 5.7. All the GA-optimized helix designs and their respective performances are presented in section 5.8 and the empirical design equations are given in section 5.9.

5.1 Introduction

Genetic algorithms are useful for optimizing helical antennas to achieve desired performances such as high gain, low axial-ratio and wide bandwidth. Previous research on the optimization of helical antennas concentrated on building and testing large numbers of designs to find optimum solutions [18-20]. Integral based numerical methods are now available to solve helical wire antennas. These methods in conjunction with modern optimization techniques such as genetic algorithms allow engineers the freedom to create antennas that meet specific radiation characteristics.

Method of moments programs such as Numerical Electromagnetics Code (NEC) decompose wire antenna structures into many segments for analysis [2]. These codes quickly analyze complex structures and determine their radiation characteristics. Information such as axial-ratio, directivity and input impedance are gathered from NEC2 for use in the desired fitness function.

The goal of the genetic algorithm in this research is to find an optimal shape for the helix that yields a low axial-ratio and high directivity over a wide bandwidth. Previous work on the helix presented new shapes and reported on their advantages and disadvantages. Genetic algorithms are used to find optimal solutions to a fitness function. Typically, GAs are used to maximize a single attribute, however a helix requires optimization of several radiation properties. The genetic algorithm must maximize directivity *and* minimize axial-ratio over a wide bandwidth. This presents a trade-off problem and thus a compromise must be made.

5.2 Shape of Helix

A conventional helix maintains a constant radius over its entire length. Variations on the axial-mode helix include tapering the radius and allowing the pitch angle to vary. Past designs include a continuous tapered helix, spherical helix, non-uniform helix and various types of envelope helices. All helix variations share a common goal of increasing the bandwidth.

The goal of this study is to use the GA to alter the radius of the helix in order to find an optimal solution for directivity and axial ratio over a wide bandwidth. A basic control over radius allows the GA to determine which, if any, of the previous designs are optimal. The GA is not limited to previous ideas and may find a unique design.

Continuously controlling the radius requires a very large number of variables to optimize. The time required to optimize hundreds of variables is not feasible. A compromise must be made to allow a discrete number of radius variables. An nth order polynomial allows n+1 discrete radius values to control the overall shape of the helix. Fitting the data in a least squares sense to a polynomial provides a simple equation to define the boundaries of the helix. The MATLAB software package has a command, ‘polyfit’, which quickly accomplishes this.

Figure 5.1 illustrates an example of a 6^{th} order polynomial fitted to the radius points. The line of the polynomial must not go below zero radii. The wire that forms the helix is guided by the polynomial. The following equations are used to find the i^{th} point along the helix path.

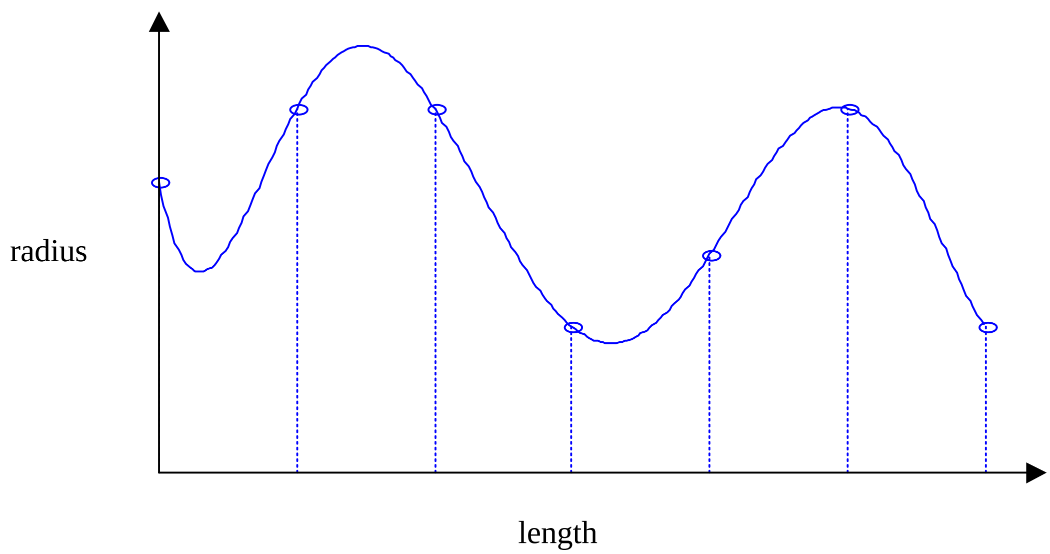

Figure 5.1: Example of 6^{th} order polynomial fitted to radius points.

$h =$ height
$N =$ number of turns
$p_j =$ jth coefficient of the nth order polynomial

$$z(i) = \frac{i \cdot h}{N \cdot seg\_turns^{*}} \tag{5.1}$$

$$r = p_1 \cdot [z(i)]^n + p_2 \cdot [z(i)]^{n-1} + \ldots + p_{n-1} \cdot [z(i)]^1 + p_n \tag{5.2}$$

$$y = 2p \frac{z(i)}{h} N \tag{5.3}$$

$$x(i) = r \cdot \cos(y) \tag{5.4}$$

$$y(i) = r \cdot \sin(y) \tag{5.5}$$

*note: seg_turns is the number of segments per turn of the helix.

Figure 5.2 shows plots of the helix design from the 6th order polynomial discussed earlier. This design is not suitable for an actual design. The example was chosen to show how higher-order polynomials are used to create different helical shapes.

In this research a second order polynomial design is chosen to define the helix shape (see figure 5.3). Using a lower order polynomial simplifies the GA optimization and maintains the general helix shape. Using higher order polynomials is very time consuming to optimize and tends to generate many helical shapes that do not radiate properly.

It is important to note that NEC2 does not allow two segments to have a bisecting angle less than ~1°. To properly connect the helix above a ground plane in NEC2 it is necessary to raise the helix a small distance above the ground plane. In this project a 0.05λ segment between the ground plane and the helix is used.

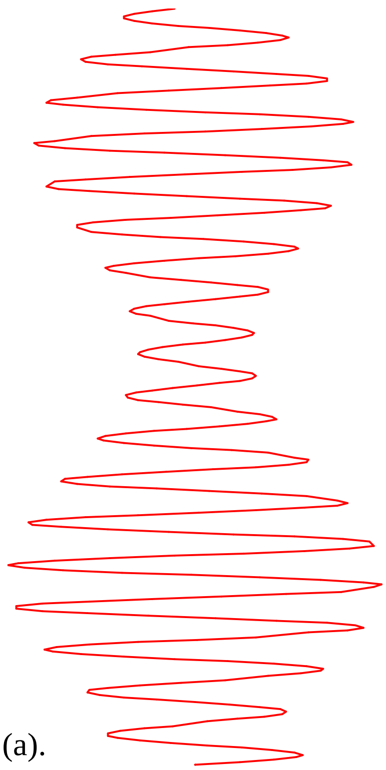

(a).

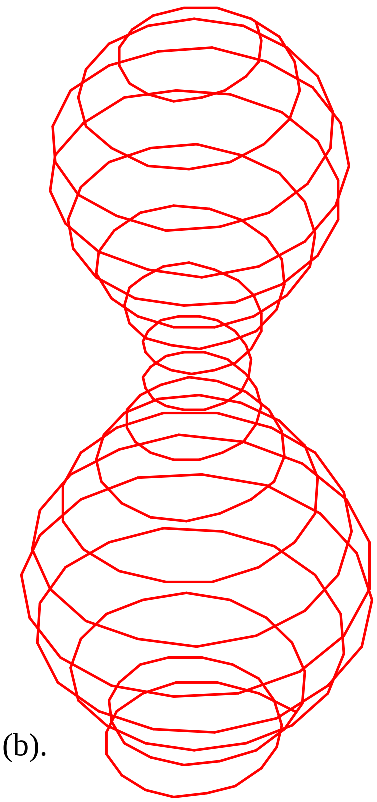

(b).

Figure 5.2: Helix obtained from a 6th order polynomial, (a) side view, (b) full view.

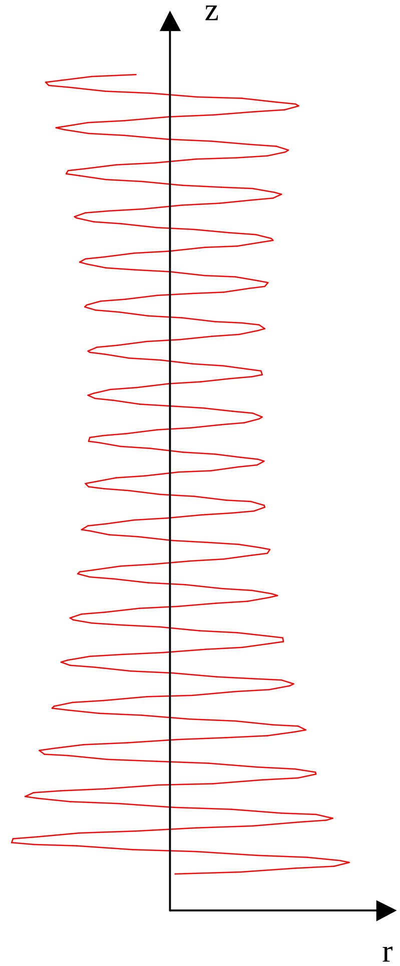

Figure 5.3: Example of 2^{nd} order polynomial (quadratic) helix.

5.3 Fitness Function

The helix has several important features. When operating in the axial mode, the helix tends to radiate circularly polarized (CP) waves. The helix is also broadband, because it is a traveling wave antenna.

In order to create an optimum shape for the helix, it is necessary to look at both directivity and axial-ratio over a wide frequency range. The GA is limited to optimizing a single fitness value. Therefore, the fitness function must be set up to intelligently characterize the selected helix shape. The method of moments code, NEC2, can accurately give both the gain and the axial-ratio in the boresight direction. In order to test over a wide bandwidth both gain and axial-ratio information must be collected over many frequencies. The gain and the axial-ratio are expressed in dB units. Over the bandwidth the axial-ratio must remain below 3dB, while the gain must not vary more than 3dB. The following examples illustrate how to generate fitness values.

5.3.1 Fitness Function: Example #1

Certain scoring criteria are utilized to better quantify the radiation characteristics of an antenna designed around a specific design frequency. While the helix does not operate at a single frequency, it is helpful to use a design frequency and the corresponding wavelength (λ) for use in generating the helix size. The length and radius are given in terms of wavelengths. It is useful to require the design frequency to lie at the center of the operating frequency range and further require that the peak gain occur at the design frequency.

The graph in Figure 5.4 illustrates how the gain and axial-ratio (AR) behaves over a wide frequency range. This particular helix would receive a score of zero because the main peak of the gain curve does not coincide with the design frequency. This scoring method is used to generate a helix that has a central design frequency reference point. Note that the AR is well below the 3dB level.

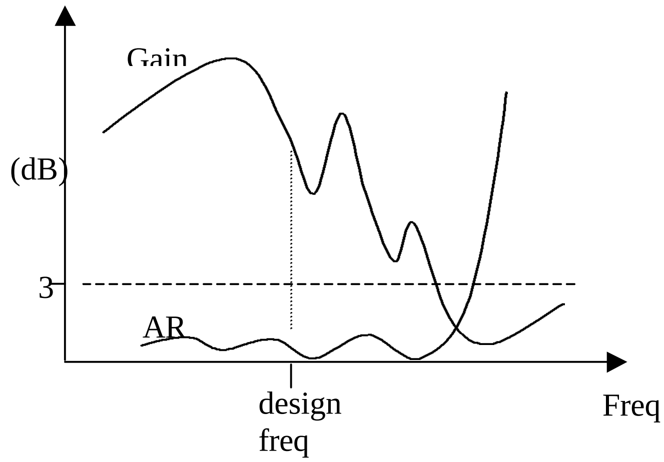

Figure 5.4: Example #1, gain and AR curves. Note that the gain curve peak is offset from the design frequency.

5.3.2 Fitness Function: Example #2

Figure 5.5 illustrates another example of the gain and axial-ratio characteristics over a wide frequency range. Notice that the gain curve peak coincides with the design frequency and the axial-ratio remains below the 3dB level. This example meets the initial performance criteria and will be fitness scored appropriately for use in the gene pool.

This second example is scored well because the design frequency coincides with the maximum gain and the axial-ratio remains below 3dB over a wide range of frequencies. In this example, the AR establishes the low frequency limit while the gain defines the upper frequency limit. The difference between these two frequencies is the bandwidth (BW). The bandwidth and the gain are used to assign a fitness value.

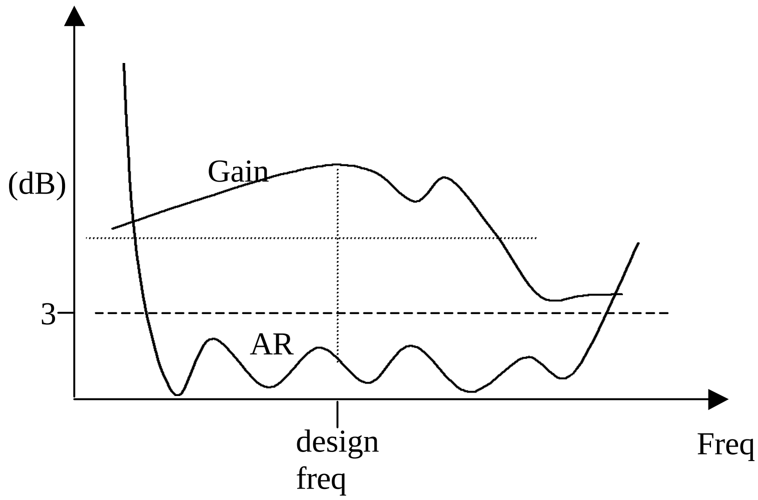

Figure 5.5: Example #2, gain and AR curves. Note that the peak gain is centered on the design frequency.

5.3.3 Fitness Function: Example #3

One problem arises when the algorithm converges to solutions that are lopsided. The GA allows the center frequency to migrate towards the lower end of the band. While this can result in relatively large bandwidths, the algorithm is merely taking advantage of the scaling difference between low and high frequency ranges. The percent bandwidth concept is ruined when the design frequency moves away from the middle of the band. An example of a lopsided gain curve is shown in Figure 5.6.

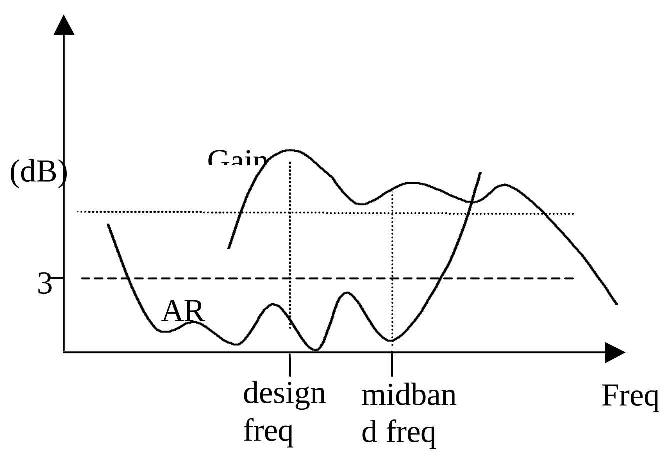

Figure 5.6: Example #3, lopsided gain and AR curves.

In this example the intended design frequency is different from the midband frequency. The midband frequency is obtained from (lower cutoff frequency) + BW/2. The percent bandwidth is defined as the ratio of bandwidth over the midband frequency. Table 5.1 illustrates a mock example of how the percent bandwidth changes.

Table 5.1: Example of lopsided percent bandwidth.

Lower freq cutoff	Upper freq cutoff	BW	Expected center freq	Midband freq	Expected %BW	Midband %BW
1.9 GHz	2.9 GHz	1 GHz	2 GHz	2.4 GHz	50%	41.6%

From this table it is noted that the algorithm is 'cheating' and, in fact, the actual percent bandwidth is smaller. To alleviate this problem, the fitness function is required to test in the following manner.

- Test the center frequency for gain and AR
- If the center frequency is acceptably large and the AR is below 3dB, continue.
- Test, in relatively small frequency steps, to the left and to the right of the center frequency.
- If both have ARs below 3dB *and* gain values that are less than 3dB below the design frequency gain, continue.
- Repeat until failure of requirements.

These procedures will yield gain curves with a peak near the design frequency. The actual results will still be slightly off-center. Even though the helix is symmetrically tested, the gain and axial-ratio performance does extend more to the higher frequency end. Therefore, the actual bandwidth will be wider than that the GA declares.

In this work, a design frequency of 2GHz and frequency steps of 50MHz are chosen. The 50MHz frequency steps values allow for bandwidths in steps of 100MHz only. Therefore, all antenna designs will have fitness values of 900 MHz, 1000 MHz, 1100 MHz and so on. With such large frequency steps many antennas will have the same fitness values. The last two digits, (00), are used to place the gain at the expected frequency. This allows the fitness values to be unique for each antenna. Table 5.2 illustrates how the fitness value is assigned.

Table 5.2: Example of fitness value calculation.

BW (MHz)	Gain (dB)	Fitness value
900	13.7	913.7
1100	12.3	1112.3
1100	13.2	1113.2
1000	14.1	1014.1

When two antennas have the same bandwidth it is clear which is superior by the fitness value. The GA can properly order the fitness of all the antennas tested using a single fitness value. The fitness value is *dimensionless*. It is merely a way of expressing two distinct values of fitness in the same statement.

5.4 GA setup

The genetic algorithm requires setup information to properly converge to an optimal solution. Table 5.3 summarizes the variables for the initial GA run.

Table 5.3: GA variable setup information for optimizing the helical antenna.

Number of variables (genes) (n)	3
Number of bits (alleles) in gene (a)	8
Number of bits in chromosome (b)	a*n = 24
Population size (N)	b*n = 72
$p_{mutation}$	0.01
$p_{crossover}$	0.7
Decimal point location (M)	-3
Selection type	Tournament
Elitist strategy	Yes

There are three variables for the coefficients of the polynomial. The height of the antenna and the number of turns are kept constant. Many different lengths and turns are tested. The probability of mutation and the probability of crossover are standard percentages determined by experimentation [6].

The rough guidelines for a conventional helix, provided by Kraus [18], maintain that the circumference of the helix should be on the order of one wavelength. Therefore, the radius should be approximately $\lambda/2\pi$ or ~0.16λ. The number of bits or alleles in the gene is 8. The decimal point location (M) is –3. These specifications in conjunction with equation (2.4) allow a maximum radius of 0.1245m or $.8306\lambda$ at 2 GHz. The selected maximum radius is well above the suggested 0.16λ. This maximum radius allows plenty of room for the GA to converge to an optimal design across a large solution space. The value of M minimizes radius step sizes to 0.000488m or 0.0033λ.

Tournament selection is used to converge towards a solution faster. Elitist strategy is used to maintain a monotonically increasing population fitness. The MATLAB code to generate the GA results can be found in the Appendix.

5.5 GA solution

The first helix to be optimized has a length of 2λ and 10 turns. After 15 generations and many hours running on a 450 MHz Pentium PC a solution was produced. The time needed to run the GA is extremely dependent on the platform used to run on and the number of segments provided for NEC2 to test the helix.

The GA created the following helix design at 2 GHz with the following radius values: $r_1 = 0.03027$ m, $r_2 = 0.02514$ m and $r_3 = 0.00756$ m. The three radius values are used to generate the polynomial coefficients using the MATLAB 'polyfit' function. Equation (5.6) and Figure 5.7 define the sides of the helix.

$$r = -0.27706 \cdot z^2 + 0.007329 \cdot z + 0.03027 \tag{5.6}$$

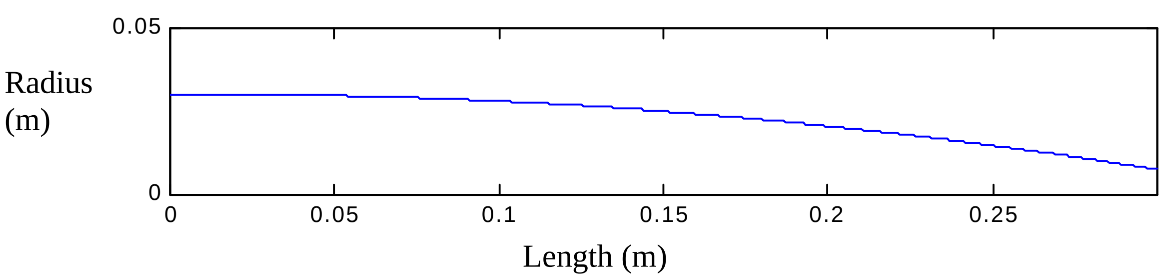

Figure 5.7 :Plot of the polynomial used to generate the GA-optimized helix envelope.

Figure 5.8 shows how the helix shape is tapered such that the circumference and the pitch angle vary along the entire length of the helix. King and Wong [19] hypothesized that this in effect increases number of wavelengths of operation due to the supported modes. Original work on the helix by Kraus [18] determined that the helix operated in the axial mode when the circumference of the helix is roughly 1.1 wavelengths and when the pitch angle is 12 – 15 degrees. The *GA-optimized* helix design covers a wide range of circumference values and pitch angles. This suggests that the helix will operate over a much wider bandwidth than the standard helix.

Varying the circumference and pitch angle is similar to the non-uniform helix design of Wong and King [22]. The non-uniform design uses discrete sections of helix lengths with differing radii and pitch angles connected by tapered sections. This non-uniform helix design produces a tapered structure that supports more modes. The GA-optimized helix does not use discrete sections. It continuously varies the circumference and the pitch angle. The continuous tapering of helix and changing of its pitch angle can be viewed from Figure 5.9. Figures 5.10 and 5.11 clearly show the changes in pitch angle and circumference along the length of the antenna.

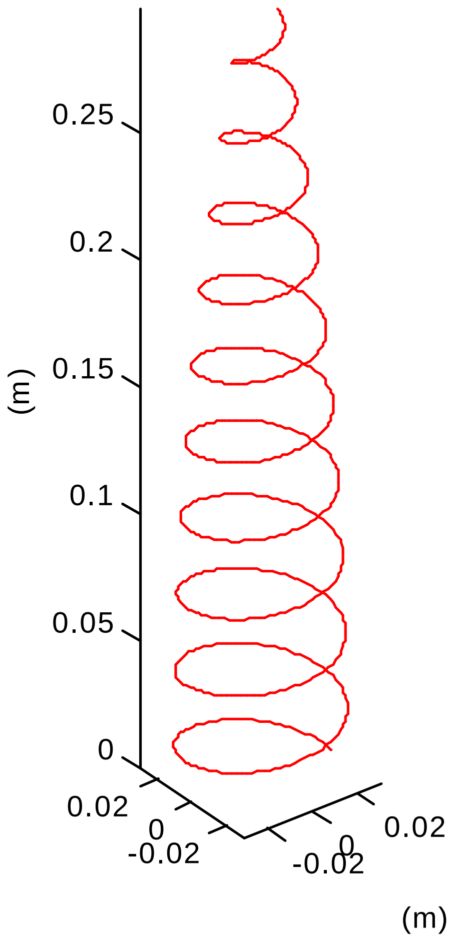

Figure 5.8: Plot of GA-optimized helix design for 2GHz. Length = 2λ, number of turns=10.

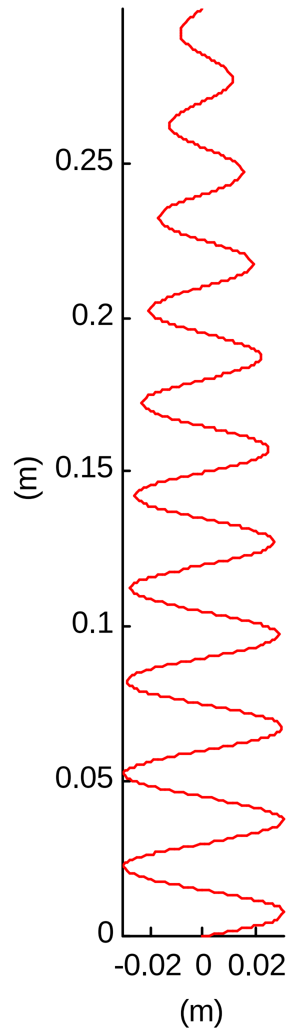

Figure 5.9: Side view of GA-optimized helix at 2GHz. Length = 2λ, number of turns=10.

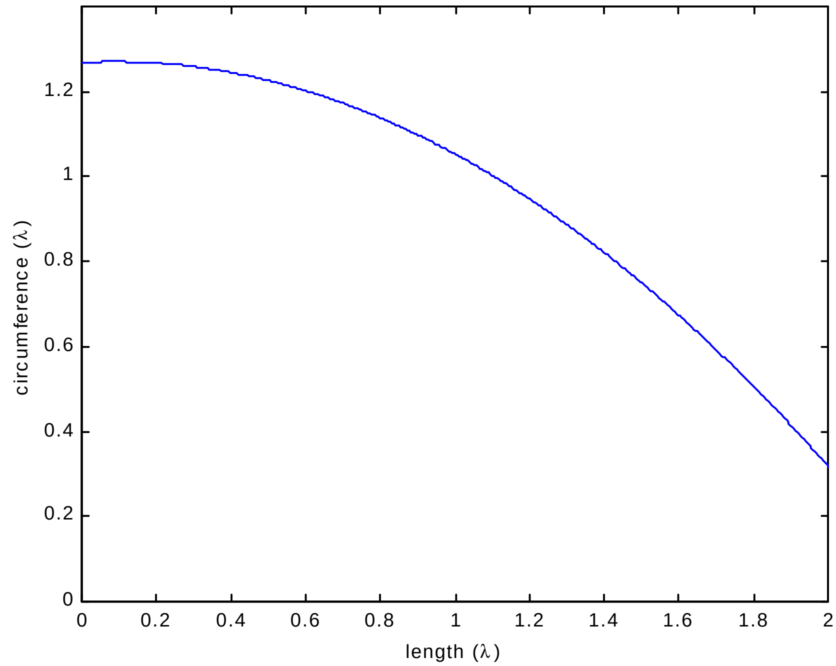

Figure 5.10: Circumference vs. length for GA-optimized helix. Note that the circumference covers a range across the suggested 1.1λ.

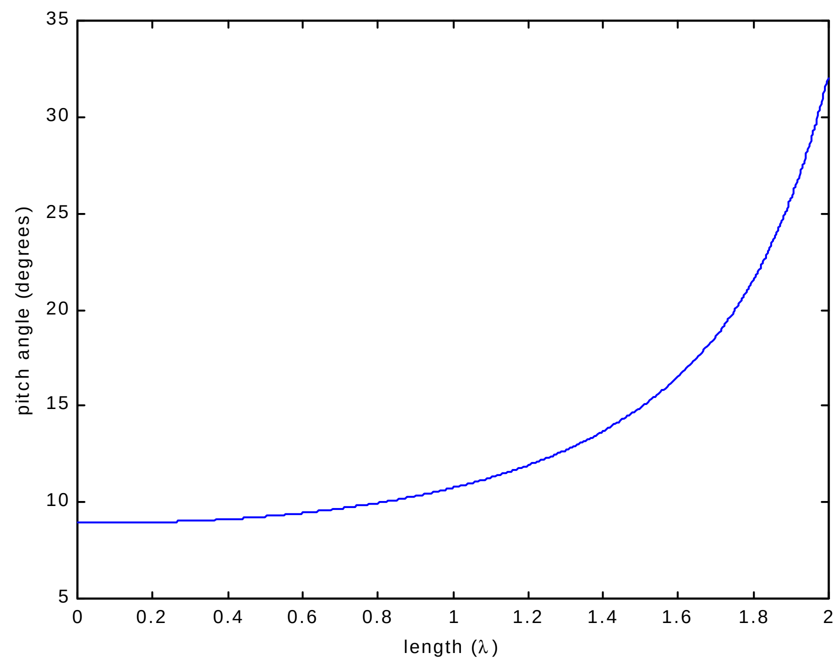

Figure 5.11: Pitch angle (α) vs. length for GA-optimized helix. Note that the pitch angle covers the suggested 11-15° range.

5.6 Performance

As expected, the GA-optimized helix design outperforms the standard helix. According to NEC2, the GA-optimized helix extends its gain response in the higher frequency range, while the standard helix gain curve drops off quite rapidly after the design frequency. Also, as noted in Figure 5.12, the GA-optimized helix provides a very low axial-ratio over a wide bandwidth. These NEC2 generated axial-ratio results are quite impressive and are among the most important characteristics for the GA-designed helix. Table 5.4 summarizes the bandwidth characteristics of this helix.

Table 5.4: Summary of GA-optimized helix performance.

Lower frequency cutoff	1400 MHz
Upper frequency cutoff	2555 MHz
Bandwidth (BW)	1155 MHz
Maximum Directivity	12.81 dB
Midband % BW (BW/midband)	58%
ratio of upper freq to lower freq	1:1.83

It is emphasized that the lower cutoff frequency is controlled by the axial-ratio frequency response, while the upper cutoff frequency is controlled by the gain characteristic. Figure 5.13 displays variations of the real part of the input impedance of the antenna. As in the case of the standard helix, the real impedance provided by NEC2 is relatively accurate. On the other hand, the NEC2 results for the imaginary part of the input impedance, shown in Figure 5.14, are not realistic.

As previously noted for the standard helix, the imaginary impedance is expected to be nearly zero. According to Figures 5.13 and 5.14, below 1400 MHz the real and imaginary impedance values oscillate rapidly. These oscillations correspond to the axial- ratio jumping up and the gain falling off.

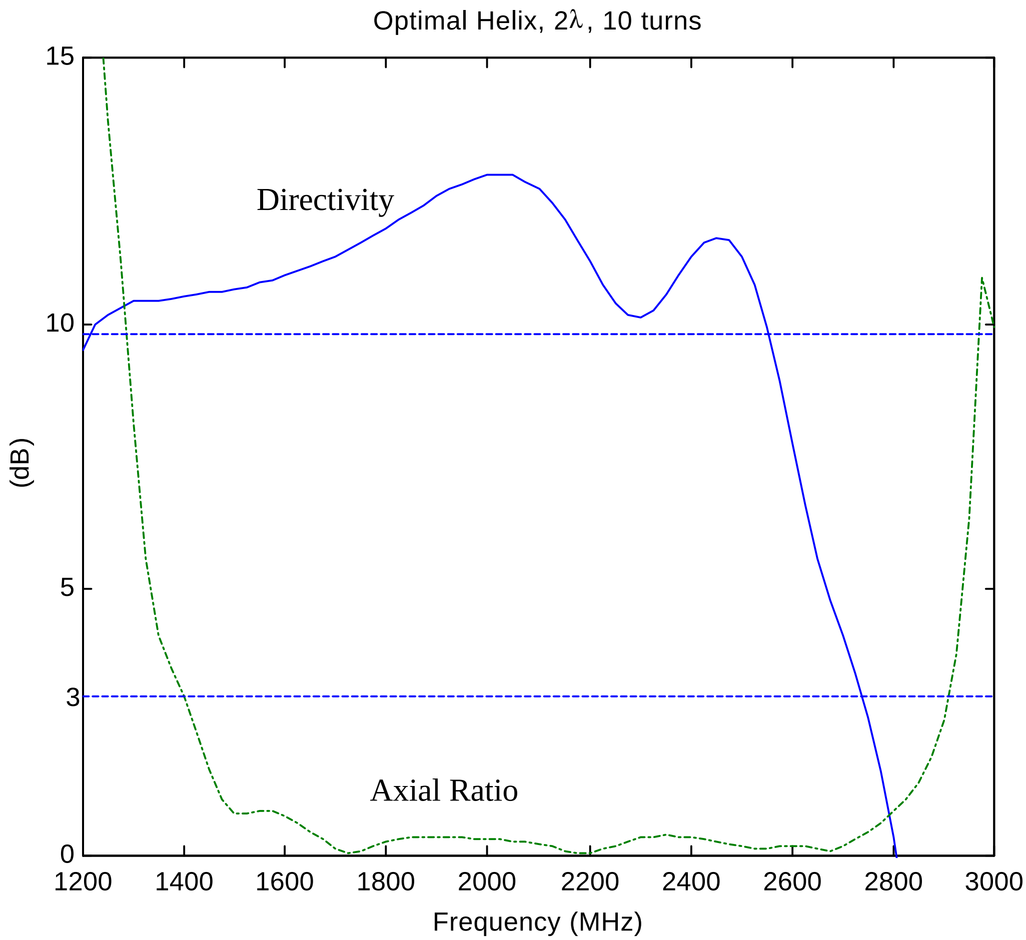

Figure 5.12: Directivity and axial ratio for 2λ, 10 turn GA-optimized helix versus frequency.

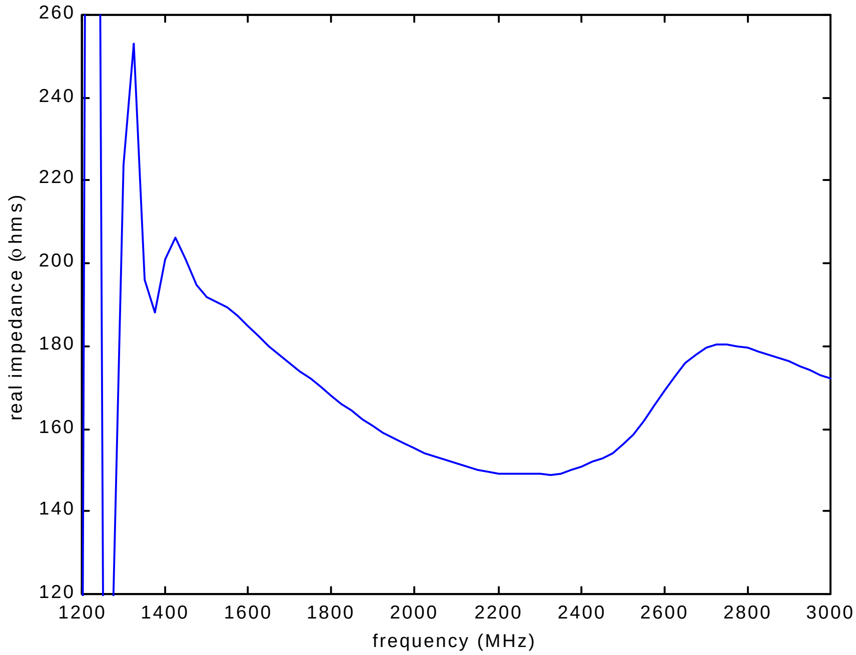

Figure 5.13: Input radiation resistance for the GA-optimized helix.

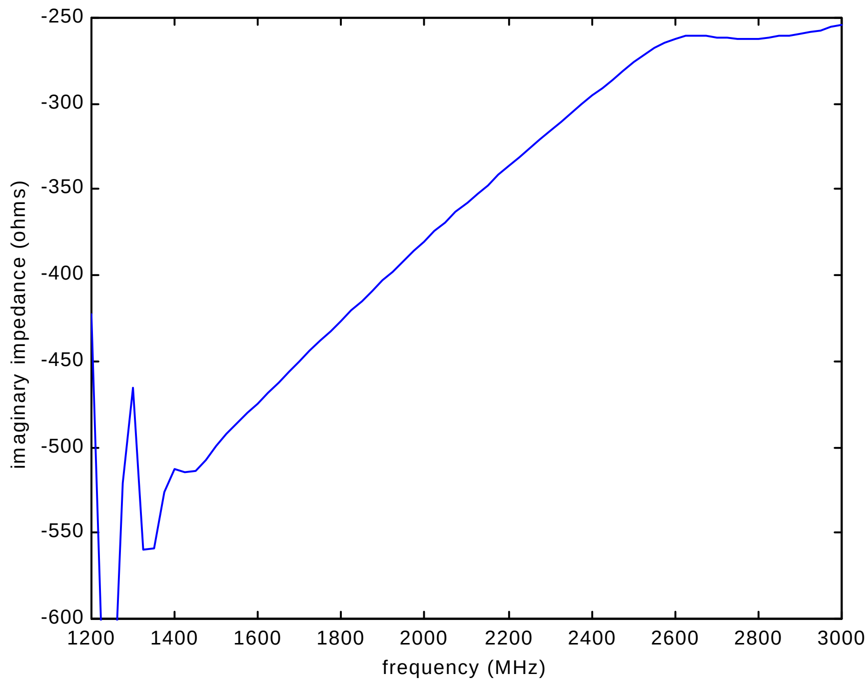

Figure 5.14: Input reactance for the GA-optimized helix.

5.7 Comparison of GA-Optimized Helix with Conventional Helix

The conventional helix design requires certain specifications to allow axial mode operation and acceptable axial-ratio and gain characteristics. The pitch angle is generally between 12 and 15 degrees, while the circumference is between 0.75λ and 1.25λ. The number of turns must be greater than 3. The height of the antenna and the number of turns and pitch angle are functions of each other.

All of the parameter ranges mentioned above have been determined by tests performed on actual helical antennas [18]. The NEC2 results are somewhat different from the measured results. For instance, the gain given by NEC2 is lower than the measured results (see Section 4.3). Factors such as ground plane type, wire diameter and feed structure all account for the differences between the calculated and measured results. The parameters of the conventional helix are given in Table 5.5.

Table 5.5: Conventional helix parameters.

Height	# of turns	radius	Circumference	pitch angle
2λ	7.5	0.0295m	1.23λ	12.13°

Optimum fitness results were produced when these parameters were used in NEC2. This conventional helix design provides the largest bandwidth for a 2λ long structure. Figure 5.15 shows the axial-ratio and directivity for both the GA-optimized and conventional helices. Visual inspection of these graphs provide insight into the advantages of the GA-optimized helix.

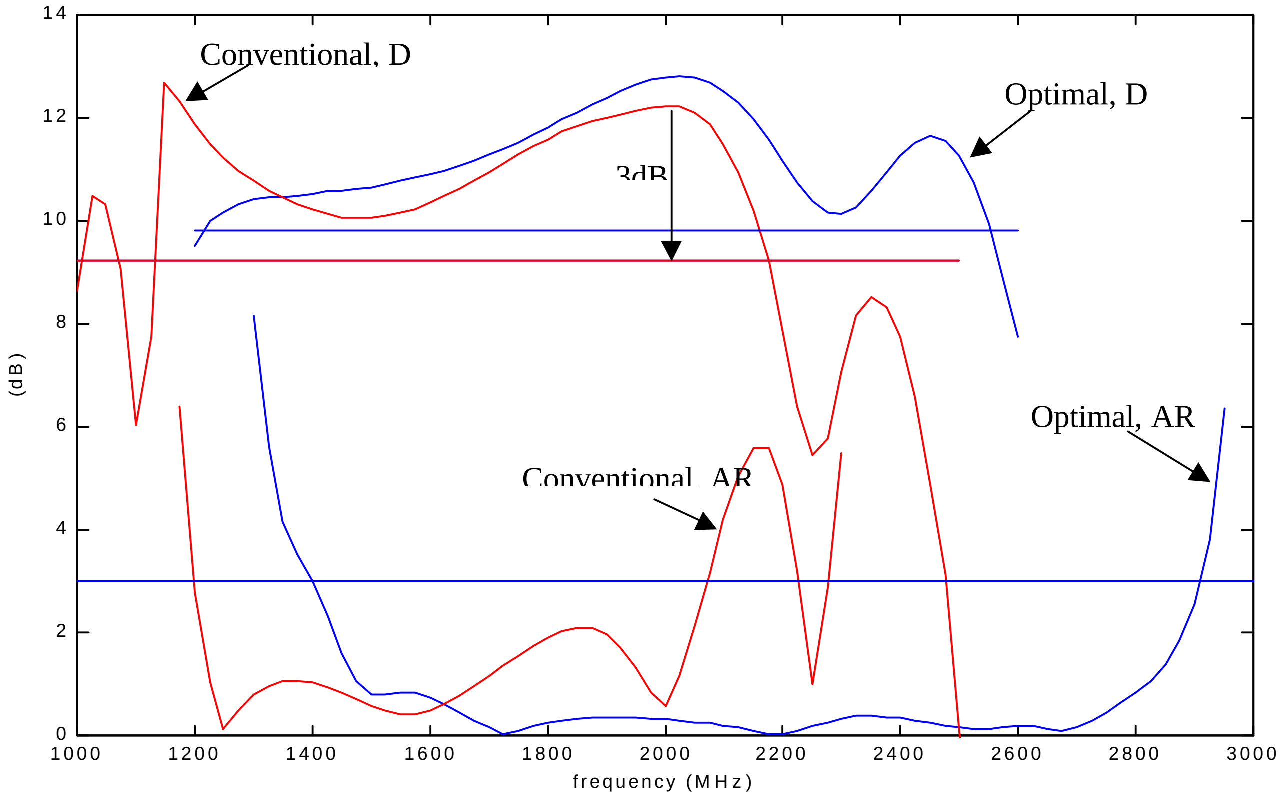

Figure 5.15: Axial ratio and gain curves for optimal and conventional helices.

The GA-optimized helix is limited in the lower frequency limited by the axial- ratio and limited in the upper frequency by the gain. The conventional helix is bandwidth limited by the axial-ratio on both sides. According to Figure 5.15, the axial-ratio appears to be the most important constraint. The axial-ratio for the GA-optimized helix is excellent over the entire range of frequencies of operation, while the axial-ratio of the conventional helix is markedly poorer than the GA-optimized helix. Table 5.6 compares the bandwidths and directivities of the conventional and GA-optimized helices.

Table 5.6 Performance of conventional versus GA-optimized helix.

Helix type:	Conventional	GA-optimized
Lower frequency cutoff	1190 MHz	1400 MHz
Upper frequency cutoff	2050 MHz	2555 MHz
Bandwidth (BW)	860 MHz	1155 MHz
Maximum Directivity	12.22 dB	12.81 dB
Midband % BW (BW/midband)	53%	58%
Ratio of upper freq to lower freq	1:1.72	1:1.83

The GA-optimized helix has 0.3dB higher directivity than the standard helix. This helix also achieves a higher percent bandwidth and frequency ratio. While these aspects are important, the lower axial-ratio is the most important characteristic.

The bandwidth of the GA-optimized helix is 25% greater than that of the conventional helix. This is misleading because the midband frequency shifts to a higher frequency. Therefore, the midband percent bandwidth term is more correct because it takes this frequency shift into account.

Figures 5.16 and 5.17 display the radiation resistance and reactance of the two helices.

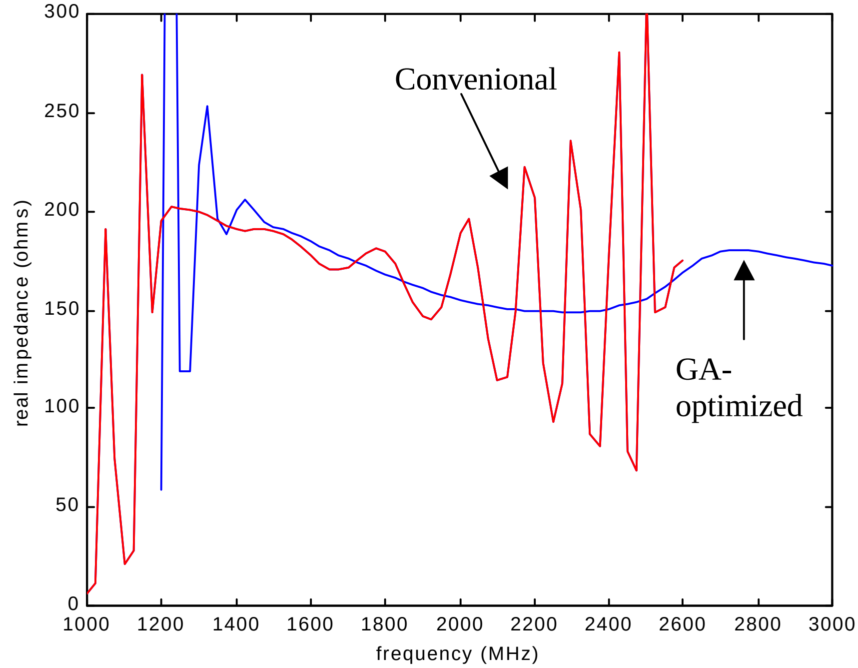

Figure 5.16: Radiation resistance of optimal and conventional helices

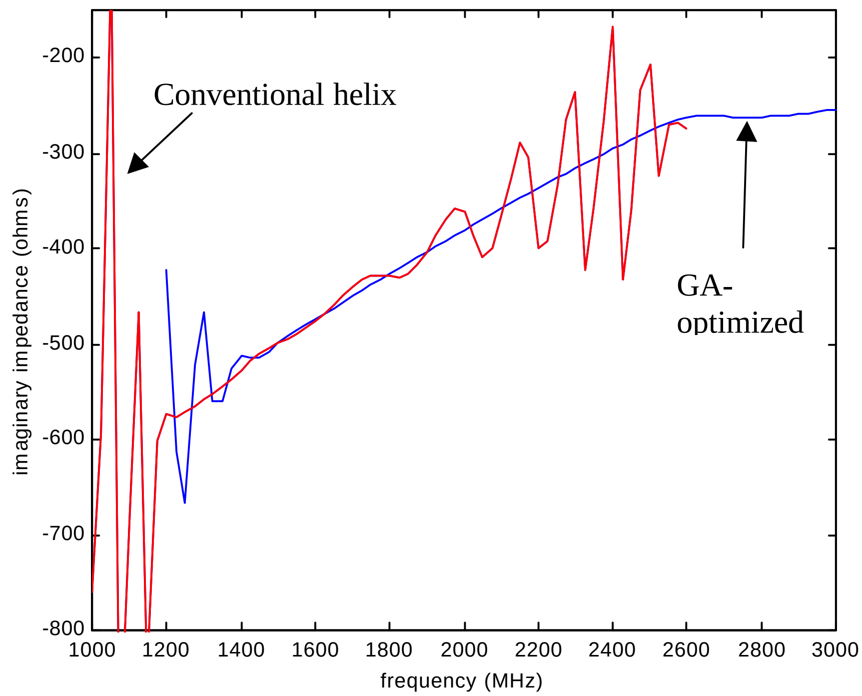

Figure 5.17: Imaginary part of the input impedance for optimal and conventional helices.

The input impedance of the GA-optimized helix tends to follow that of the conventional helix. The impedance of the GA-optimized helix does not oscillate as much across the frequency band. This indicates a wider operating region.

Another way to compare the GA-optimized helix to the conventional helix is to define a GA-optimized helix with roughly the same performance as the conventional helix and compare the sizes of the two helices. For example, using a 2λ, 7.5-turn conventional helix it is possible to compare it to a GA-optimized 1λ, 12-turn helix and a 0.5λ, 12-turn GA-optimized helix.

Table 5.7 Comparison of a conventional helix to other GA-optimized helices.

Helix type:	2λ, 7.5 turn Conventional	1λ, 12 turn GA-optimized	0.5λ, 12 turn GA-optimized
Lower frequency cutoff	1190 MHz	1750 MHz	1970
Upper frequency cutoff	2050 MHz	3005 MHz	3245
Bandwidth (BW)	860 MHz	1285 MHz	1275
Maximum Directivity	12.22 dB	11.77 dB	10.34
Midband % BW (BW/midband)	53%	54%	49%
Ratio of upper freq to lower freq	1:1.72	1:1.75	1:1.65

It is apparent from Table 5.7 that gain of the GA-optimized helices is lower than the conventional helix. This is because the two GA-optimized helices are 2 and 4 times smaller than the conventional helix. It is important to see that a 1λ GA-optimized helix actually outperforms a 2λ conventional helix in bandwidth and axial-ratio. The 0.5λ GA-optimized helix does not quite meet the specifications but is displayed to show how robust the design is compared to the conventional helix. This 0.5λ helix is 400% smaller than the conventional helix but loses only 2.2dB in gain and 4% in bandwidth.

5.8 Complete Solutions

Optimization runs on the helix were performed for lengths of 1λ, 1.5λ, 2λ, 2.5λ and 3λ. Each length was run with numbers of turns ranging from 6 to 24. A very large data set was accumulated and analyzed. Table 5.8 contains a subset of the helices tested.

Table 5.8 GA-optimized helix spreadsheet.

L	N	f_l	f_u	D	BW	BW/f_o	f_u/f_l	r_1 (m)	r_2 (m)	r_3 (m)
0.5	4	1670	2495	9.96	825	40%	1.49	0.0303	0.0251	0.00757
0.5	6	1900	2770	10.11	870	37%	1.46	0.0294	0.0244	0.00734
0.5	8	1935	2950	10.2	1015	42%	1.52	0.0285	0.0236	0.00711
0.5	10	1940	3100	10.25	1160	46%	1.60	0.0275	0.0229	0.00689
0.5	12	1970	3245	10.34	1275	49%	1.65	0.0266	0.0221	0.00666
1	4	1540	2480	11	940	47%	1.61	0.0312	0.0259	0.0078
1	6	1585	2395	11.49	810	41%	1.51	0.0303	0.0251	0.00757
1	8	1620	2665	11.62	1045	49%	1.65	0.0294	0.0244	0.00734
1	10	1665	2845	11.72	1180	52%	1.71	0.0285	0.0236	0.00711
1	12	1720	3005	11.77	1285	54%	1.75	0.0275	0.0229	0.00689
1	14	1775	3160	11.85	1385	56%	1.78	0.0266	0.0221	0.00666
2	6	1300	2345	12	1045	57%	1.80	0.0321	0.0267	0.00802
2	8	1345	2345	12.51	1000	54%	1.74	0.0312	0.0259	0.0078
2	10	1400	2555	12.81	1155	58%	1.83	0.0303	0.0251	0.00757
2	12	1435	2705	13.06	1270	61%	1.89	0.0294	0.0244	0.00734
2	14	1490	2745	13.22	1255	59%	1.84	0.0285	0.0236	0.00711
2	16	1555	2900	13.35	1345	60%	1.86	0.0275	0.0229	0.00689
2	18	1615	3050	13.45	1435	62%	1.89	0.0266	0.0221	0.00666
2	20	1670	3100	13.56	1430	60%	1.86	0.0257	0.0214	0.00643
2	22	1735	3260	13.66	1525	61%	1.88	0.0248	0.0206	0.00621
2	24	1810	3425	13.76	1615	62%	1.89	0.0239	0.0199	0.00598

3	12	1280	2445	13.39	1165	63%	1.91	0.0312	0.0259	0.0078
3	14	1320	2530	13.68	1210	63%	1.92	0.0303	0.0251	0.00757
3	16	1375	2635	13.9	1260	63%	1.92	0.0294	0.0244	0.00734
3	18	1430	2775	14.08	1345	64%	1.94	0.0285	0.0236	0.00711
3	20	1475	2835	14.23	1360	63%	1.92	0.0275	0.0229	0.00689
3	22	1540	2980	14.37	1440	64%	1.94	0.0266	0.0221	0.00666
3	24	1600	3120	14.5	1520	64%	1.95	0.0257	0.0214	0.00643
3	26	1650	3200	14.62	1550	64%	1.94	0.0248	0.0206	0.00621

A commonality between the GA-optimized and the conventional helix is the gain characteristic. As the height and number of turns increase the gain increases. This result is not at all unusual. As the structure length (both actual height and wire length) is increased, less power is reflected from the top of the helix back to the receiver, and, more of the signal is transmitted. This is common to traveling wave, broadband antennas.

The results in Table 5.8 reveal an interesting trend that appears to be unique to the GA-optimized helix. As the number of turns increases the bandwidth also increases. The conventional helix suffers from loss of bandwidth as the numbers of turns increases, because the constant pitch angle falls well below 12°.

The better bandwidth performance can be attributed to the varying pitch angle and circumference. The wide bandwidth is due to the varying circumference values that support many different frequencies. Increasing the number of turns does not significantly affect the pitch angle because the pitch angle varies all along the length of the helix. Therefore, increasing the number of turns merely increases the gain and does not decrease the bandwidth.

The bandwidth increase effect is negated by the shift of the band. A closer look at the BW versus %BW columns shows that as the number of turns increases, the BW increases *but* the % BW stays relatively constant. This is due to *both* the lower and the upper cutoff points shifting up.

The three radius values for each case also show simple trends. As the number of turns increases each radius value decreases. Also, as the height increases the radius increases. These values are linearly related, allowing empirical relations to be derived from these trends.

Figure 5.18 illustrates the directivity and axial-ratio for a 3λ helical antenna for varying number of turns. Again, it is observed that the axial-ratio sets the lower frequency cutoff while the directivity limits the upper frequency. Note that all antennas have a peak gain at 2 GHz. The 2 GHz peak is used as the design frequency. Each helix design always has its gain peak occuring at the frequency of operation (i.e. 2 GHz). Therefore, when the length or radius is listed in units of wavelengths (λ), the wavelength corresponds to the peak of the gain curve.

Note that for this 3λ tall helix the axial-ratio is excellent. The AR stays below 0.5dB over the entire bandwidth for all cases. Also, note that the gain increases with the number of turns. The number of extended oscillations of the gain curve increases as the numbers of turns increase.

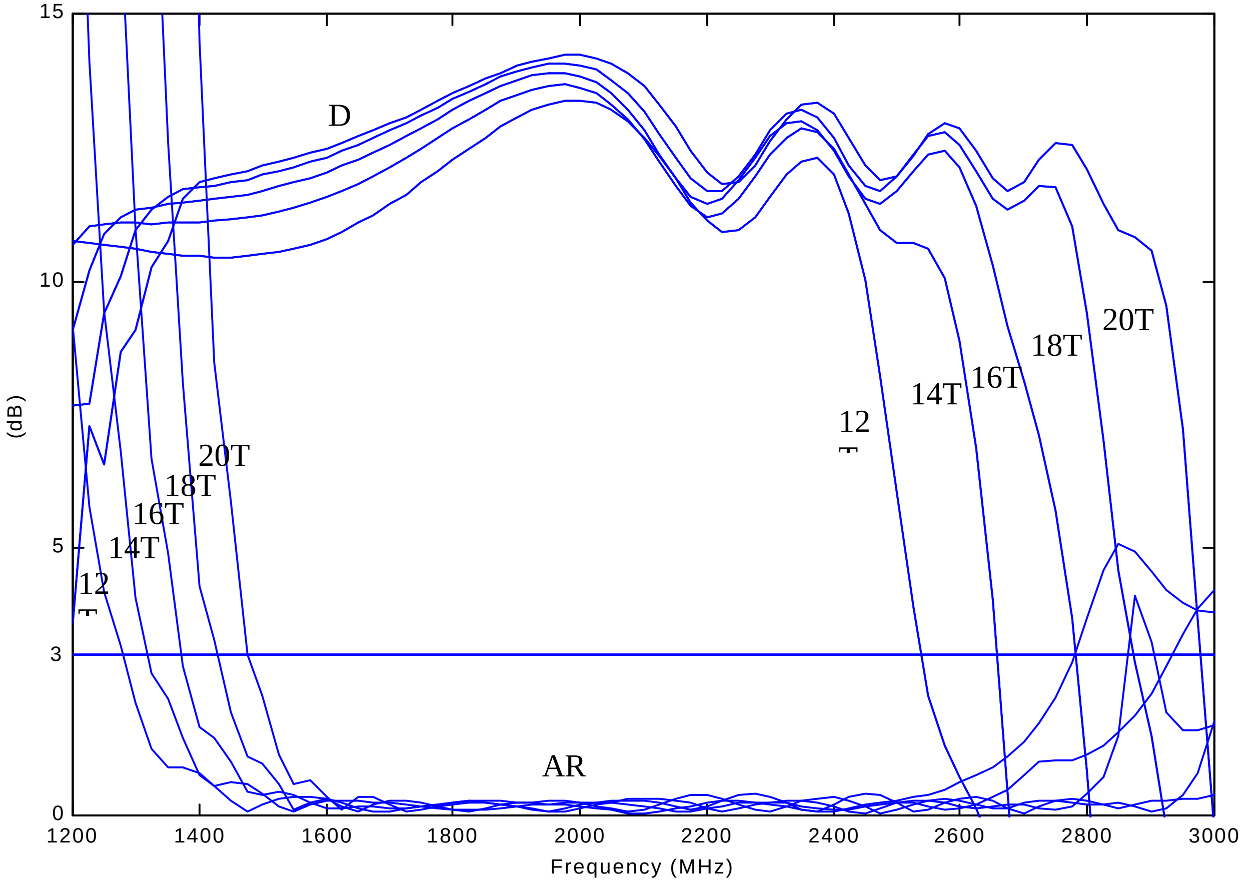

Figure 5.18: Directivity and axial ratio for a 3λ helix with varying turns.

5.9 Empirical Design Equations

The following design equations are based on the data collected from many runs of the GA for many cases. They are listed relative to number of turns (T) and height (h). The height value, h, is listed with respect to λ. Therefore, there are no units for height and number of turns.

$$r_1 = \left(0.201954 + \left(2 + 4 \cdot h - N\right) \cdot 0.0030293\right) \cdot l \qquad (5.7)$$

$$r_2 = \left(0.167752 + \left(2 + 4 \cdot h - N\right) \cdot 0.0025163\right) \cdot l \qquad (5.8)$$

$$r_3 = \left(0.050487 + \left(2 + 4 \cdot h - N\right) \cdot 0.0007573\right) \cdot l \qquad (5.9)$$

$$p_1 = \frac{-0.1711102 - 0.00996758 \cdot h + 0.0024919 \cdot N}{l \cdot h^2} \qquad (5.10)$$

$$p_2 = \frac{0.0150979 + 0.00087949 \cdot h - 0.00021987 \cdot N}{h} \qquad (5.11)$$

$$p_3 = \left(0.2080163 + 0.0121174 \cdot h - 0.0030294 \cdot N\right) \cdot l \qquad (5.12)$$

In these equations $r(0) = r_1$, $r(h/2) = r_2$ and $r(h) = r_3$. Also, p_n, for n=1, 2, and 3, are the coefficients of the quadratic equation that defines the helix shape (see section 5.2, equation 5.2). Equations (5.7 to 5-12) all are valid for $h \geq 0.5$ and $N \geq 8$.

Chapter 6 Far-Field Measurements of the GA-Optimized Helix Antenna

A 12-turn, 2λ high GA-optimized helix antenna was constructed and tested on the Virginia Tech antenna range. The helical antenna was designed to operate between 1.6GHz and 3.4GHz, which is well within the operating limits of the Virginia Tech antenna range. The power pattern was obtained by taking E_θ and E_φ planar cuts. The multiple-amplitude method was used to obtain the axial-ratio of the antenna. Section 6.1 discusses the method of construction for the helical antenna. Section 6.2 overviews the measurement process as well as the method used to find the axial-ratio. A comparison of the measured patterns versus the simulated NEC2 results is presented in Section 6.3.

6.1 Antenna Construction

A 2λ, 12-turn GA-optimized helical antenna with a design midband frequency of 2.6GHz was constructed for use in the measurement campaign. A suitable construction method is necessary to accurately make the antenna. Strict construction tolerances are needed to properly compare the measured data to the simulated NEC2 results. The following discussion overviews the antenna geometry and the construction methods used.

6.1.1 Antenna Geometry

All sizes and specifications must be obtained to make the antenna. At a design frequency of 2.6GHz, the wavelength (λ_d) of operation is 11.531cm. Therefore, the $2\lambda_d$ long helical antenna is 23.06cm tall. The wavelength, $\lambda_{d,}$ is used in conjunction with equations (5.7) to (5.12) to define the coefficients of the quadratic equation that characterizes the envelope of the GA-optimized helix. Substituting λ_d = 0.1153 into (5.7) to (5.12), we obtain

$$r_1 = (0.201954 + (2 + 4 \cdot 2 - 12) \cdot 0.0030293) \cdot 0.1153 = 0.02258m \tag{6.1a}$$
$$r_2 = (0.167752 + (2 + 4 \cdot 2 - 12) \cdot 0.0025163) \cdot 0.1153 = 0.01876m \tag{6.1b}$$
$$r_3 = (0.050487 + (2 + 4 \cdot 2 - 12) \cdot 0.0007573) \cdot 0.1153 = 0.005647m \tag{6.1c}$$

$$p_1 = \frac{-0.1711102 - 0.00996758 \cdot 2 + 0.0024919 \cdot 12}{0.1153 \cdot 2^2} = -0.349375 \tag{6.2a}$$
$$p_2 = \frac{0.0150979 + 0.00087949 \cdot 2 - 0.00021987 \cdot 12}{2} = 0.0071092 \tag{6.2b}$$
$$p_3 = (0.2080163 + 0.0121174 \cdot 2 - 0.0030294 \cdot 12) \cdot 0.1153 = 0.022588 \tag{6.2c}$$

$$r(i) = -0.349375[z(i)]^2 + 0.0071092z(i) + 0.022588 \tag{6.3}$$

Equation (6.1) provides the radius values at the base, the middle and the top of the antenna. These radii give a general impression of the size of the antenna, as well as a confidence value to compare to the quadratic equation (6.3). Equation (6.1) shows that the radius of the antenna is 2.25cm at the base and tapers down to a radius of 0.5cm at the top. Equation (6.2) provides the coefficients of the quadratic equation (6.3). These equations are empirical results derived from the GAs solution sets in Chapter 5.

The antenna was constructed such that it matches, as closely as possible, the model used to obtain the simulation results. For example, the antenna is raised $0.05\lambda_d$ above the ground plane (as explained in Chapter 4) and a wire radius of 0.25mm is used in order to try and match the simulated NEC2 results.

6.1.2 Construction Method

The path of the wire to create the helix shape can be obtained using equation (6.3) in conjunction with equations (5.1) to (5.5). The height of the antenna is $2\lambda_d$ or 23.06cm. This, combined with the $0.05\lambda_d$ spacing above the ground plane provides a total structural height of 23.64cm. The following construction method is very simple and allows relatively close agreement between the hand-built antenna and the helix path defined by the above equations.

Balsa wood is used for the inner support structure because it is very easy to cut and mark. Balsa wood is also very dry and light and thus provides dielectric properties that are similar to air. Using several thin pieces of balsa wood and a small amount of glue allows a structure support that is mainly comprised of air. For this project, $1/8^{th}$ inch thick balsa wood and super glue are used for the construction of the support structure.

The first step in creating the support structure is to cut out three equally sized pieces of balsa wood that are 23.64cm tall and whose sides conform to equation (6.3). Figure 6.1 illustrates the general appearance of the three pieces of prepared balsa wood. Then, using equations (5.1) to (5.5), allow the variable *seg_turns* to have a value of 6. This will provide individual values of ρ and z at $\varphi = 0°, 60°, 120°, 180°, 240°$, and $300°$.

Figure 6.1a illustrates how these ρ and z values should be marked at $\varphi = 0°$. The wood pieces should be appropriately marked based on their respective angles. Next, appropriate cuts out of the inside of each piece are made. This allows the three pieces to fit on top of each other as a type of 3-D puzzle. Once placed together, super glue is used to lock the pieces together. It is important to keep each piece exactly 60° apart in order to retain the correct path of the helix. If the pieces are not 60° apart, the pitch angle within the incorrectly angled section will not correspond to the pitch angle of the GA-optimized helix.

The markings on the side of each piece correspond to the location on which the wrapped wire should lie. Each marking is notched so that the wire will stay within the marking while a dab of super glue is applied. Note that NEC2 specifies wire location based at the center of the wire. Therefore, the notches in the balsa wood should be as deep as the wire radius, 0.25mm. Figure 6.2 shows the final structure with the wire appropriately wrapped around it.

A ground plane should be fitted below the helix structure. The metal ground plane should be at least 0.75λ across at the antennas lowest frequency of operation [18]. In this project a pie pan was fashioned below the antenna. The pan is 18cm across which corresponds to a diameter of one wavelength at 1.6GHz. The pie pan has sides that turn up with a maximum height of 3cm. Figure 6.3 displays the actual antenna that was built and tested on the Virginia Tech antenna range.

This method helps to make the construction process as accurate as possible. Still, achieving the exact radius at all locations is quite difficult. If the actual radius of the structure varies, the expected gain and axial ratio plots will be shifted left or right with respect to frequency. For example, at a design frequency of 2.6 GHz, if the helix radius is only 1mm too large, then the actual design frequency will be 2.5 GHz and the bandwidth will shift 100 MHz to the left.

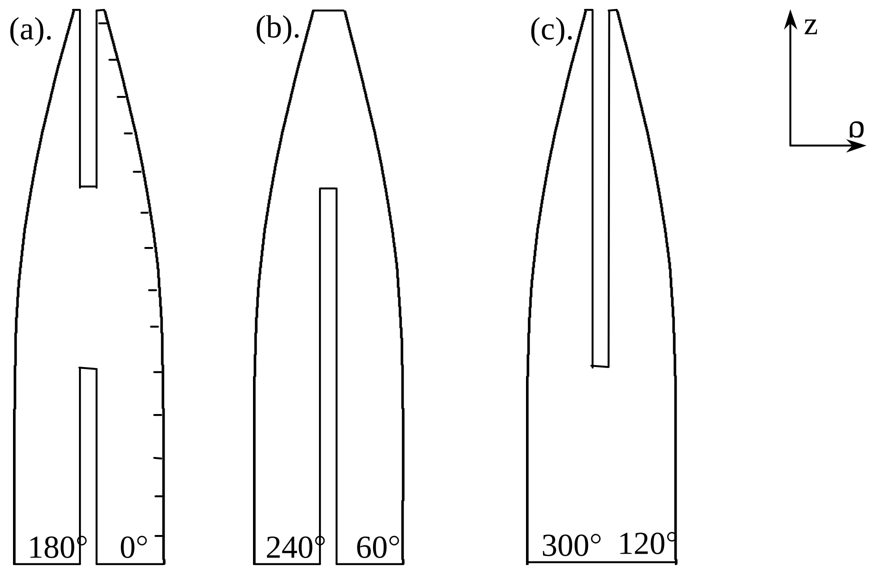

Figure 6.1: Templates for helix support

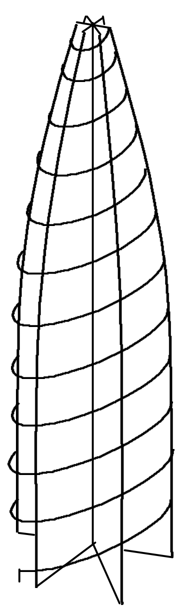

Figure 6.2: Antenna structure with wire helix wrapped around it.

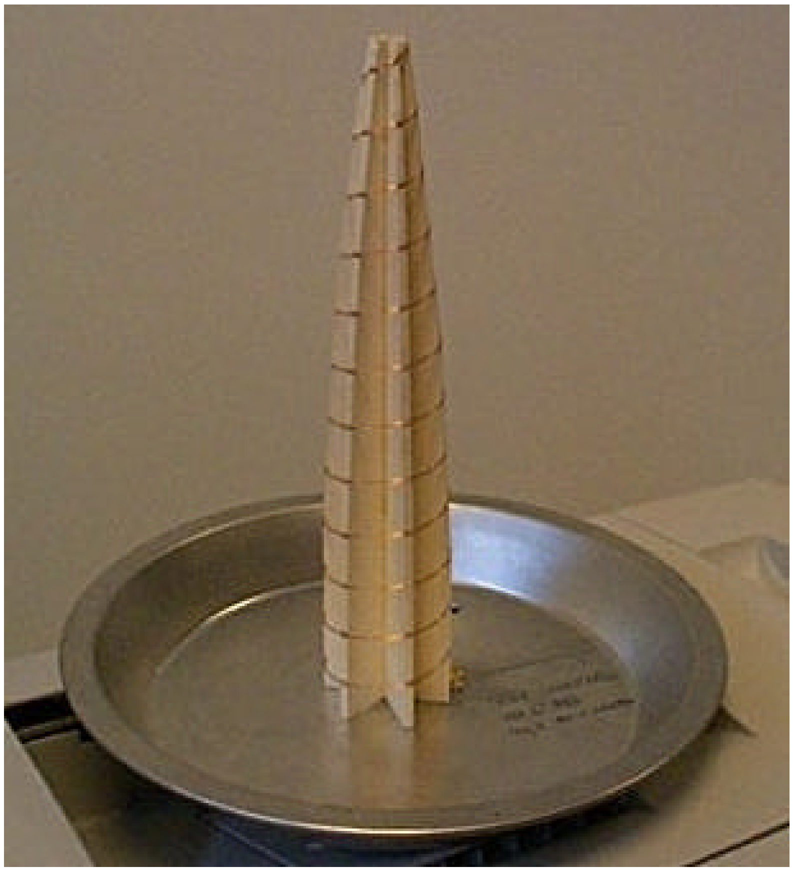

Figure 6.3 Photograph of the actual GA-optimized helix built.

6.2 Measurements Procedures

The constructed GA-optimized helix was tested on the Virginia Tech antenna range. The antenna range allows relative amplitude measurements to be taken over a range of frequencies and azimuth and elevation angles. By rotating the transmitter antenna (see Figure 6.4), pattern cuts at $\theta = 0°$, 45°, 90° and 135° are taken. At each setting of the transmitter antenna, the test antenna is azimutally rotated through 360 degrees in 2 degree increments. Relative amplitude measurements were taken in 100MHz steps between 1.6GHz and 3.6GHz.

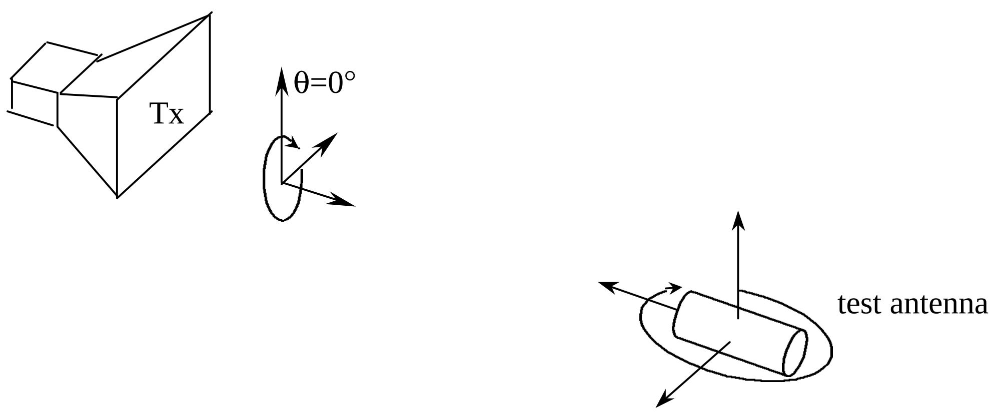

Figure 6.4 Antenna measurement setup.

Power patterns are calculated by taking the E_θ ($\theta = 0°$) and E_φ ($\theta = 90°$) components and properly combining them using the following relation,

$$E_{total} = \sqrt{\left|E_\theta\right|^2 + \left|E_\varphi\right|^2}\ . \qquad (6.8)$$

Axial-ratio is obtained using the multiple-amplitude method [29]. The time varying electric field of a circularly polarized (CP) wave traces out a perfect circle. No antenna produces a perfectly CP wave and the polarization is generally elliptical. The axial-ratio, defined as the major axis to minor axis of the polarization ellipse, is used as a measure of how close to circular polarization the radiated wave of the designed antenna is.

Four amplitude points are needed to define the shape of an ellipse. The four amplitude components are measured at θ = 0°, 45°, 90° and 135°. They are then used to determine the axial-ratio following the procedure outlined below. First, amplitude ratios are calculated,

$$|r_L| = \frac{E_0}{E_{90}} \quad \text{ratio of vertical to horizontal components} \tag{6.5}$$

$$|r_D| = \frac{E_{135}}{E_{45}} \quad \text{ratio of } 135^\circ \text{ to } 45^\circ \text{ components} \tag{6.6}$$

From these ratios we can define

$$Y_L = \frac{1-|r_L|^2}{1+|r_L|^2} \tag{6.7}$$

$$Y_L = \frac{1-|r_D|^2}{1+|r_D|^2} \tag{6.8}$$

These values are used in (6.9) and (6.10) to find the axial ratio of the antenna.

$$l_m = \frac{1}{2}\cos^{-1}\left[\sqrt{Y_L^2 + Y_D^2}\right] \tag{6.9}$$

$$AR = 20\log_{10}\left(|-\cot(l_m|\right) \tag{6.10}$$

The polarization of the antenna is considered nearly circular if the AR quantity is below 3dB. A propagating wave is perfectly circular polarized if the AR is zero and the wave is linearly polarized if the AR is infinity.

6.3 Measurement Results

The far-field measurement campaign yielded power patterns and axial-ratio information for comparison with the NEC2 simulated results. The measurements taken provide relative amplitudes and do not declare actual antenna gains. For this reason, only a power pattern comparison can yield proper simulation verification. Figure 6.5 illustrates the gain and axial-ratio performance that is expected from the GA-optimized helix. In Figure 6.5 the axial ratio is plotted at the boresight (0°) and at 10°, 20°, 30°, and 40° off the boresight. This is done to show that the axial ratio should provide circular polarization off of the main beam direction (0°).

The antenna that was built and tested has a different ground plane than the simulated antenna ground plane. The NEC2 ground plane is an infinite perfectly conducting plane, whereas the built antenna uses a pie pan with up turned sides. The pie pan is approximately 18cm in diameter with a height of 3cm. In order to properly compare the NEC2 results to the actual measured results, it is necessary to generate a ground plane in NEC2 that replicates the pie pan shape. Using virtual patches of perfect conductor, a pie pan was pieced together. Figure 6.6 shows a drawing of actual NEC2 model for the complete antenna structure. Using the input data file for this model, the resulting NEC2 patterns are compared against the measured data.

Figures 6.7 through 6.11 display the patterns that were measured on the Virginia Tech antenna range versus the simulated results. The simulated results closely match the measured results at most all frequencies. The main beam and sidelobe structure match very well. The back lobe structures as well as the front to back lobe ratio of the measured patterns closely agree with the simulated patterns. This suggests that the radiation characteristics of the built antenna should match the predicted results obtained from the NEC2 results.

Figure 6.12 displays the half power beamwidth of the simulated and measured patterns across the bandwidth. The beamwidth between the simulated and measured patterns differ by only 2 or 3 degrees from 1.6 GHz to 3.2 GHz. The beamwidth information is not correct passed 3.2 GHz because the patterns do not have a defined mainlobe.

No impedance information was gathered for built antenna. Therefore, it is only presumed that if the antenna is properly impedance matched across the bandwidth that gain of the antenna would stay within 3dB. This is a reasonable assumption considering the relatively flat input resistance response of the simulated antenna as seen in Figure 5.16.

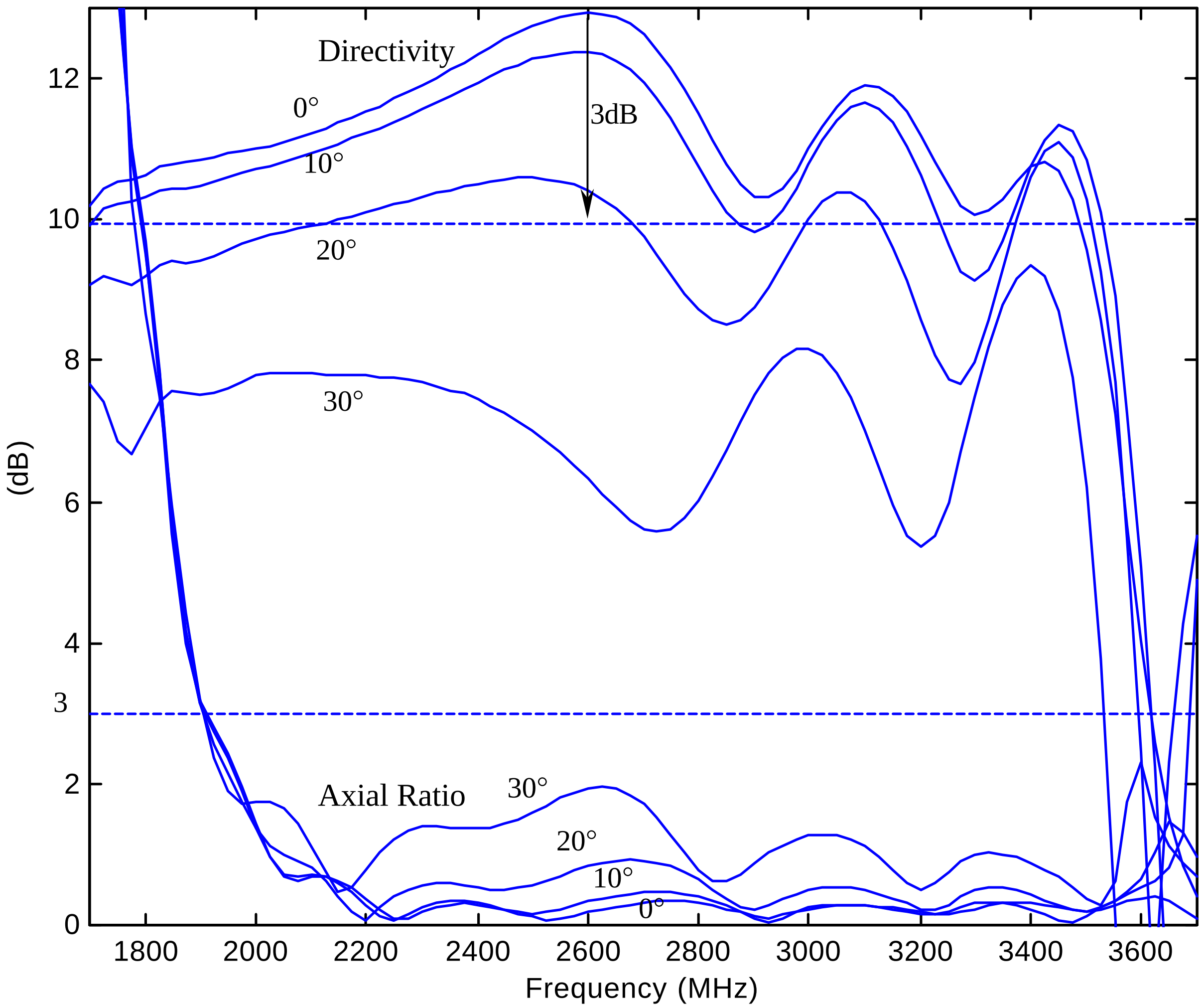

Figure 6.5 Directivity and axial ratio of 2λ, 12 turn GA-optimized helix.

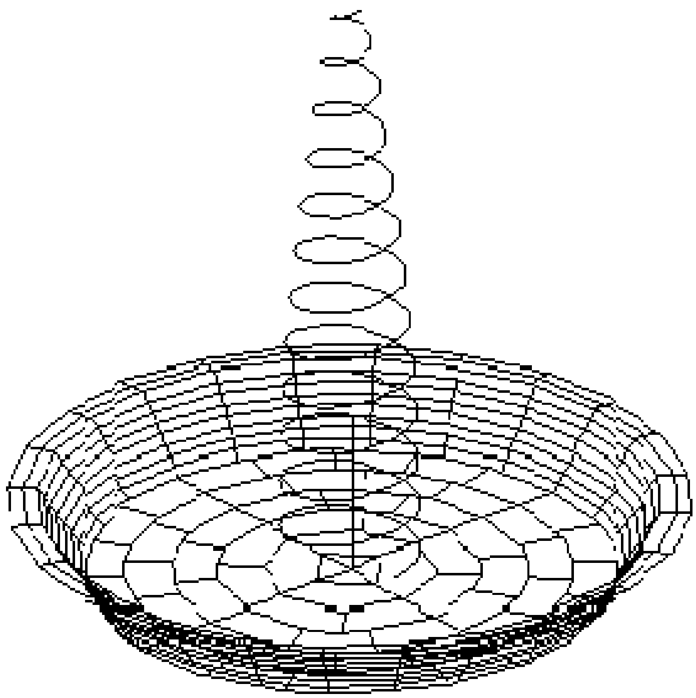

Figure 6.6: NEC2 wire input file.

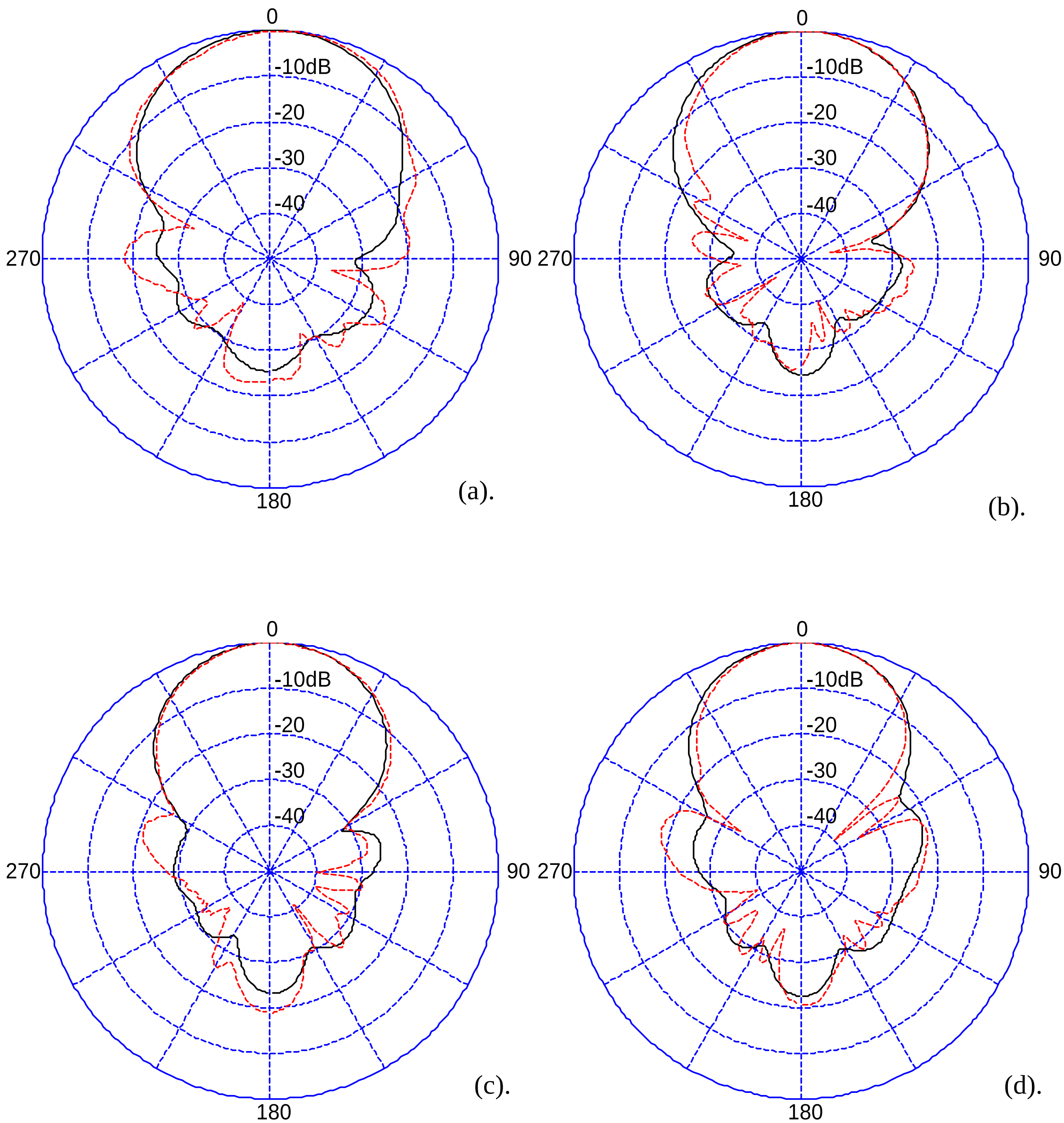

Figure 6.7 Measured (dashed line) versus simulated (solid line) power patterns at: (a). 1.6 GHz, (b). 1.7 GHz, (c). 1.8 GHz, and (d). 1.9 GHz.

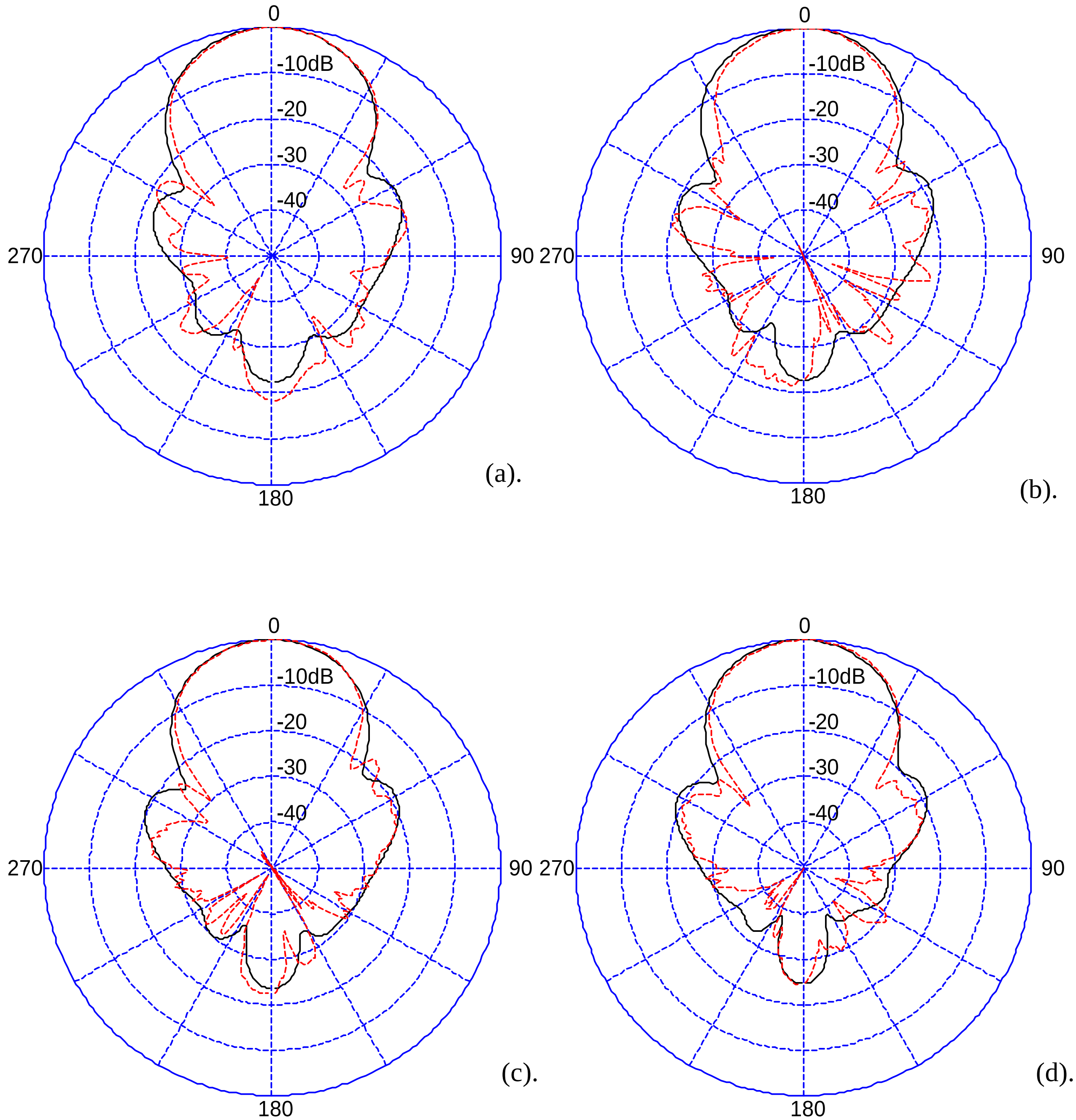

Figure 6.8 Measured (dashed line) versus simulated (solid line) power patterns at: (a). 2.0 GHz, (b). 2.1 GHz, (c). 2.2 GHz, and (d). 2.3 GHz.

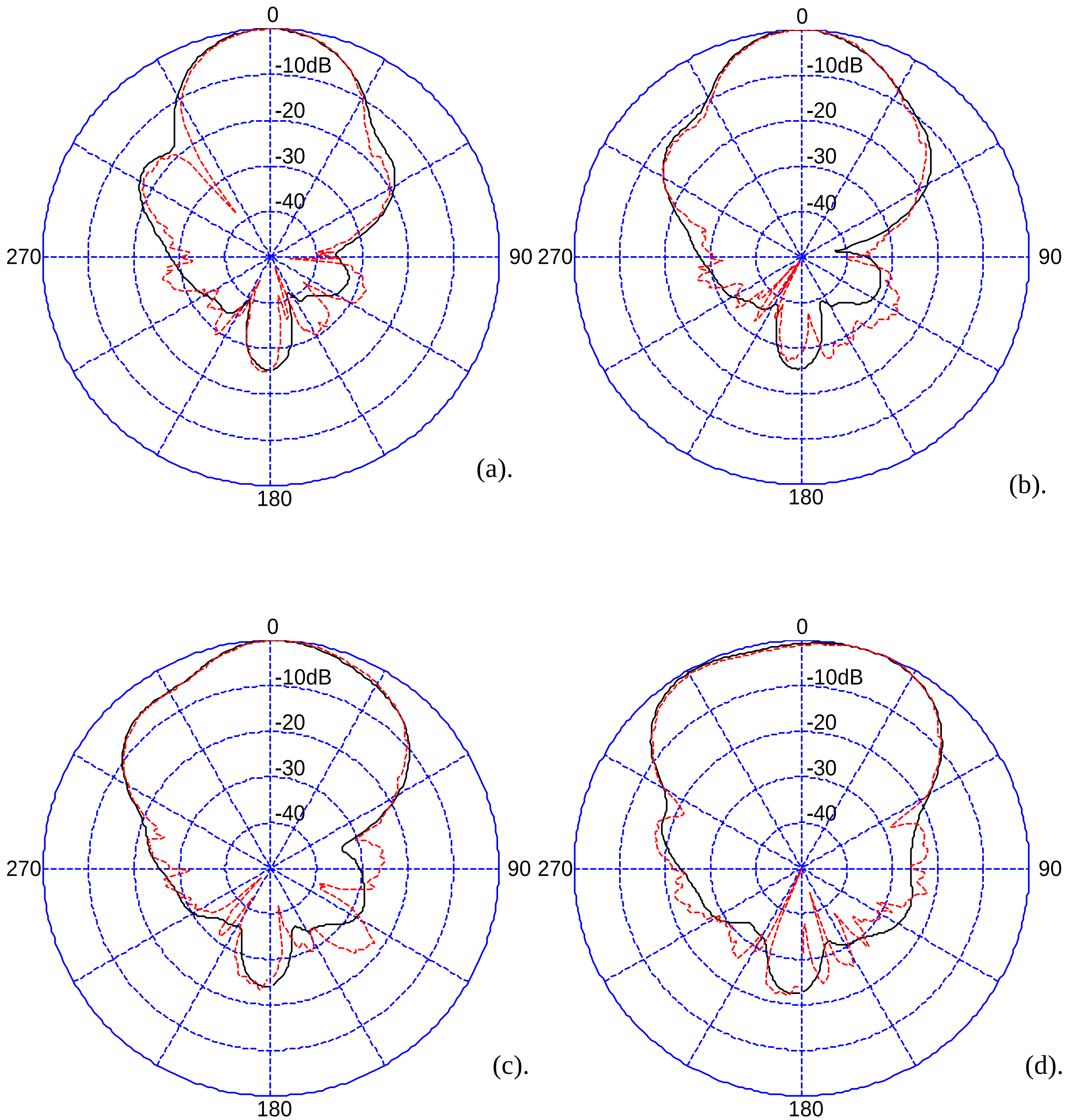

Figure 6.9 Measured (dashed line) versus simulated (solid line) power patterns at: (a). 2.4 GHz, (b). 2.5 GHz, (c). 2.6 GHz, and (d). 2.7 GHz.

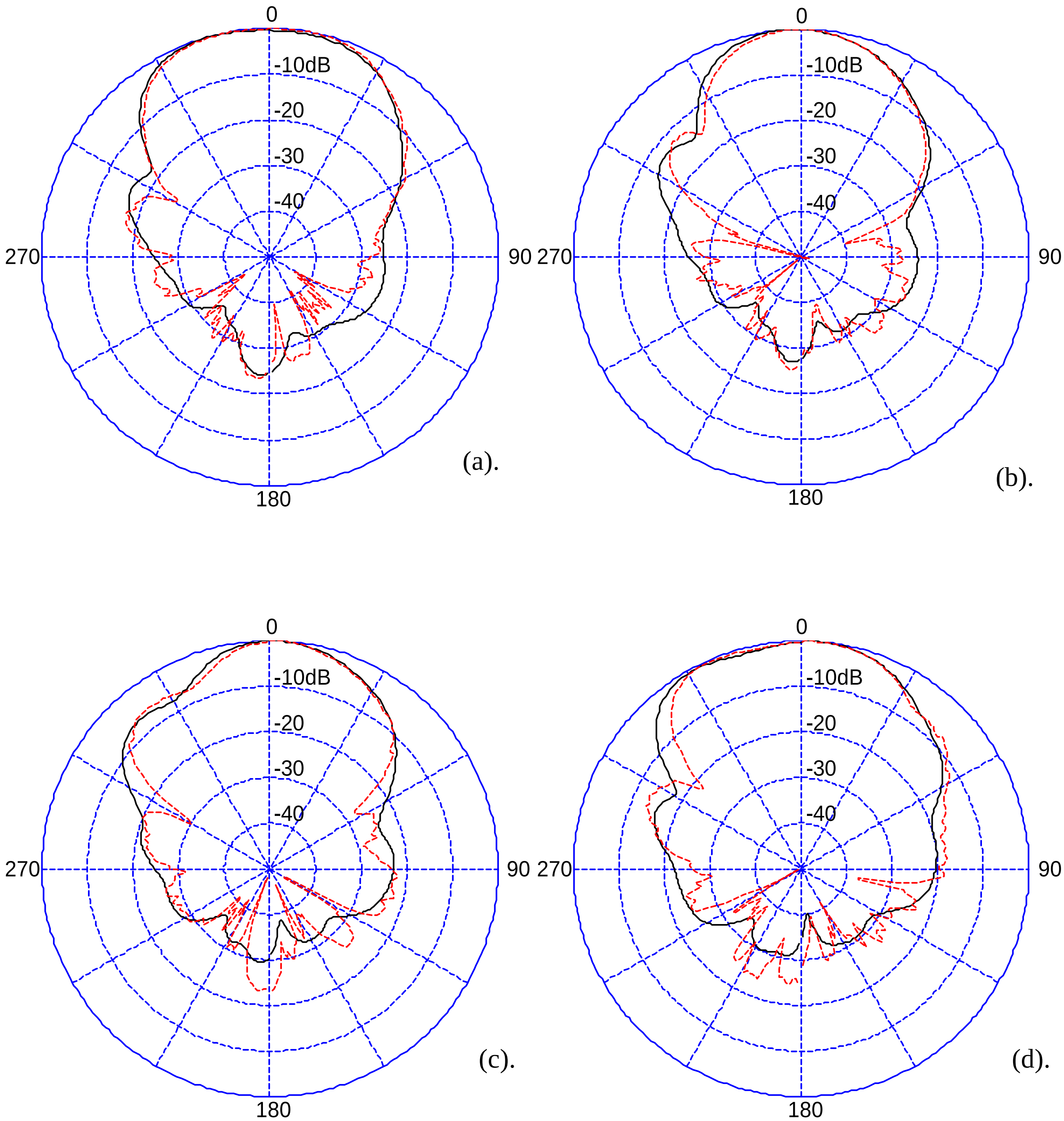

Figure 6.10 Measured (dashed line) versus simulated (solid line) power patterns at: (a). 2.8 GHz, (b). 2.9 GHz, (c). 3.0 GHz, and (d). 3.1 GHz.

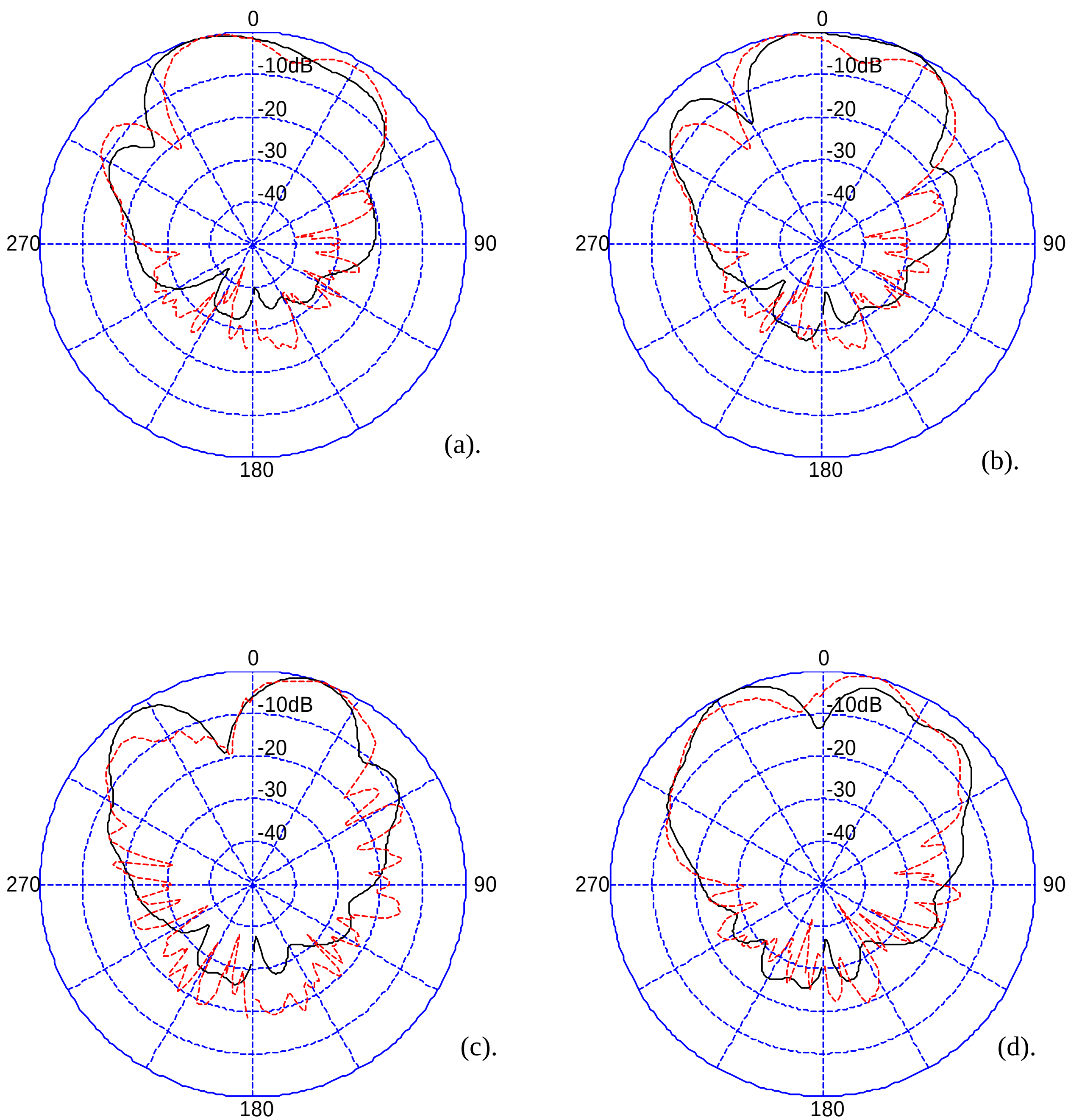

Figure 6.11 Measured (dashed line) versus simulated (solid line) power patterns at: (a). 3.2 GHz, (b). 3.3 GHz, (c). 3.4 GHz, and (d). 3.5 GHz.

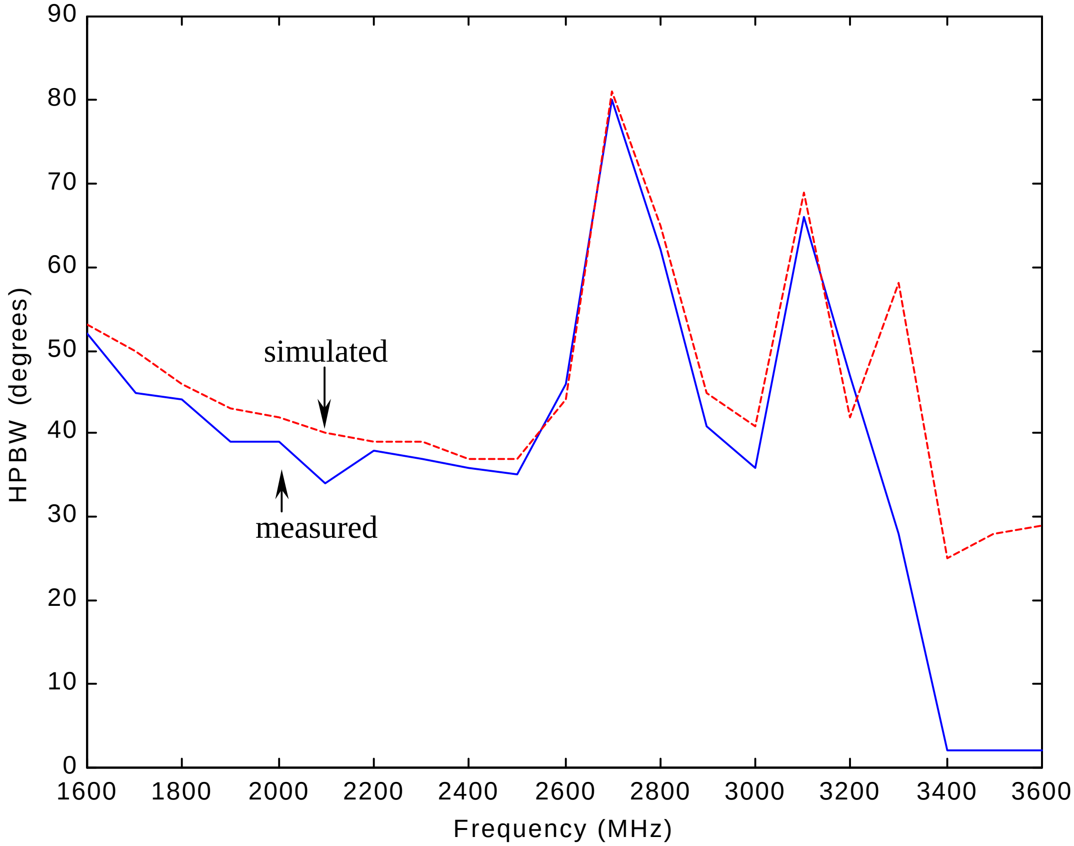

Figure 6.12 The half-power beamwidth of the simulated and measured GA-optimized helix antennas.

Figure 6.14 shows the measured axial-ratio across the bandwidth of the antenna. The axial-ratio generally stays below 3dB, which indicates that the wave produced by the antenna is circularly polarized. The measured axial-ratio does not closely match the simulated axial-ratio. This can be attributed to a number of measurement procedure complications.

The antenna range on the roof of Whittemore Hall is situated in such a way that allows both direct and specular reflections off of the walls and roof. Figure 6.13 illustrates the relative antenna range setup and displays the possible paths that the transmitted wave can travel. These received waves travel different distances and thus have different phases when they reach the test antenna. This received signal would not cause significant problems in the main beam direction if the transmitting antenna transmitted a symmetric beam towards the test antenna. Problems arise when the rectangular standard gain horn is tilted on its axis to 45°, 90° and 135°. Since the pattern of the standard horn is not rotationally symmetric, different power levels can be received at the test antenna. The axial-ratio calculations are sensitive to differences in received power levels at the different transmitter settings. Therefore it is hypothesized that the axial ratio calculations are not accurate due to these signal reflections.

The method used to calculate the axial-ratio requires amplitude information at four transmitter antenna angles (see Equations 6.9-10). At each transmitter antenna position the test antenna is azimuthally spun around to cut a pattern. The test antenna is initially 'eyeballed' to see if it is pointing directly at the transmitting antenna. Once the antenna is positioned, a device spins the test antenna in 2° increments. These increments are not accurate; in fact the device first moves what it believes to be 2° and then records the actual azimuth angle. The actual angle is never measured at exactly 2-degree increments. Wind can also slightly shift the test antenna back and forth.

This procedure turns out to work fine when the main beam is relatively wide and symmetric about the boresight. This is because the relative gain of the antenna should not vary across the boresight. Problems arise when the maximum gain moves away from the boresight. For instance, close inspection of the patterns at 3.2 GHz and above shows that peak of the beam does not coincide with the axial direction. In fact the beam is beginning to split or bifurcate near the boresight. These nulls causes great swings in power levels at the boresight and accurate amplitude information is nearly impossible to gather near these nulls. Errors in antenna alignment coupled with wind interference and test antenna rotation error account for some of the perceived errors in axial ratio calculations above 3.2 GHz.

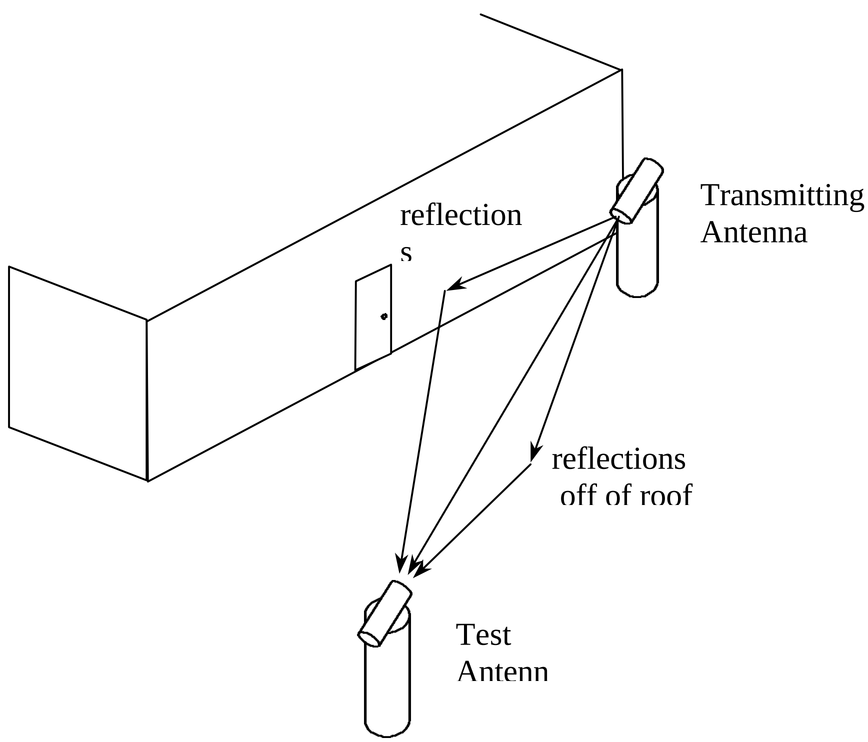

Figure 6.13 Antenna test range on the top of Whittemore with signal reflections off of roof and walls.

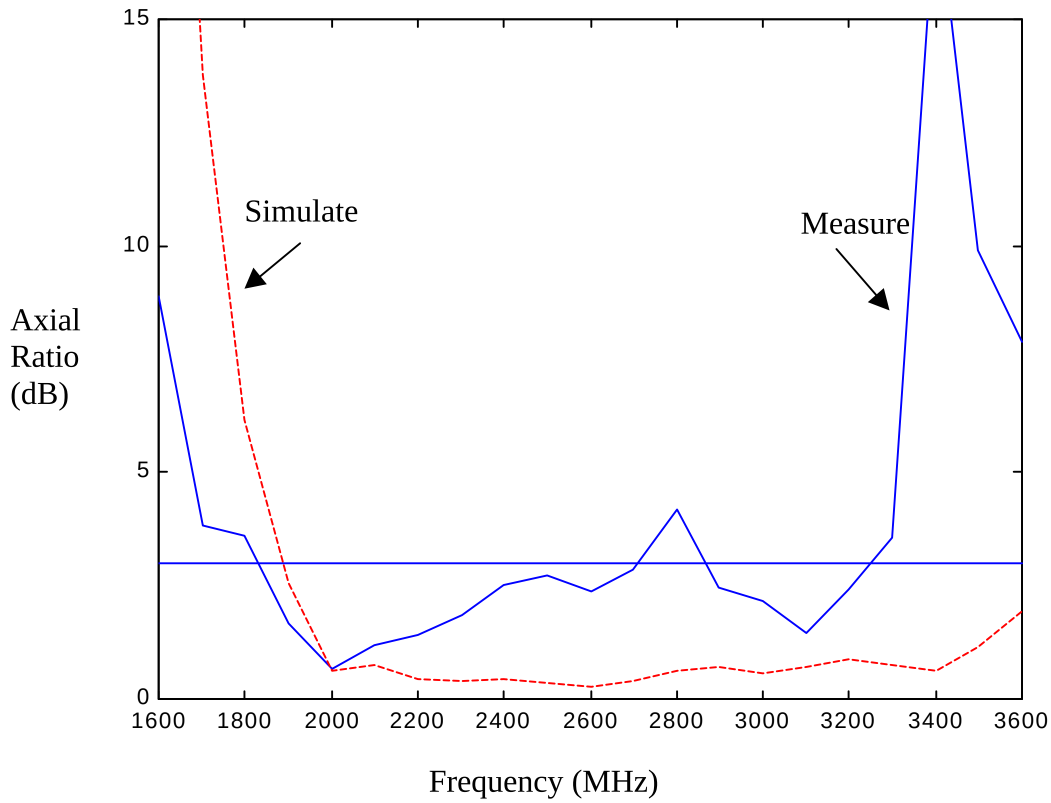

Figure 6.14: Measured and simulated axial-ratios.

Figure 6.15 displays the axial ratio at 0°, 10°, and 20° off of the boresight. It is difficult to compare the measured axial-ratio to the simulated axial-ratio in Figure 6.5. The axial-ratio in Figure 6.5 gently increases as the angle off the boresight increases. In this measured case, the lines of the measured axial-ratio data off of the boresight tend to jump around the boresight axial-ratio in a random pattern.

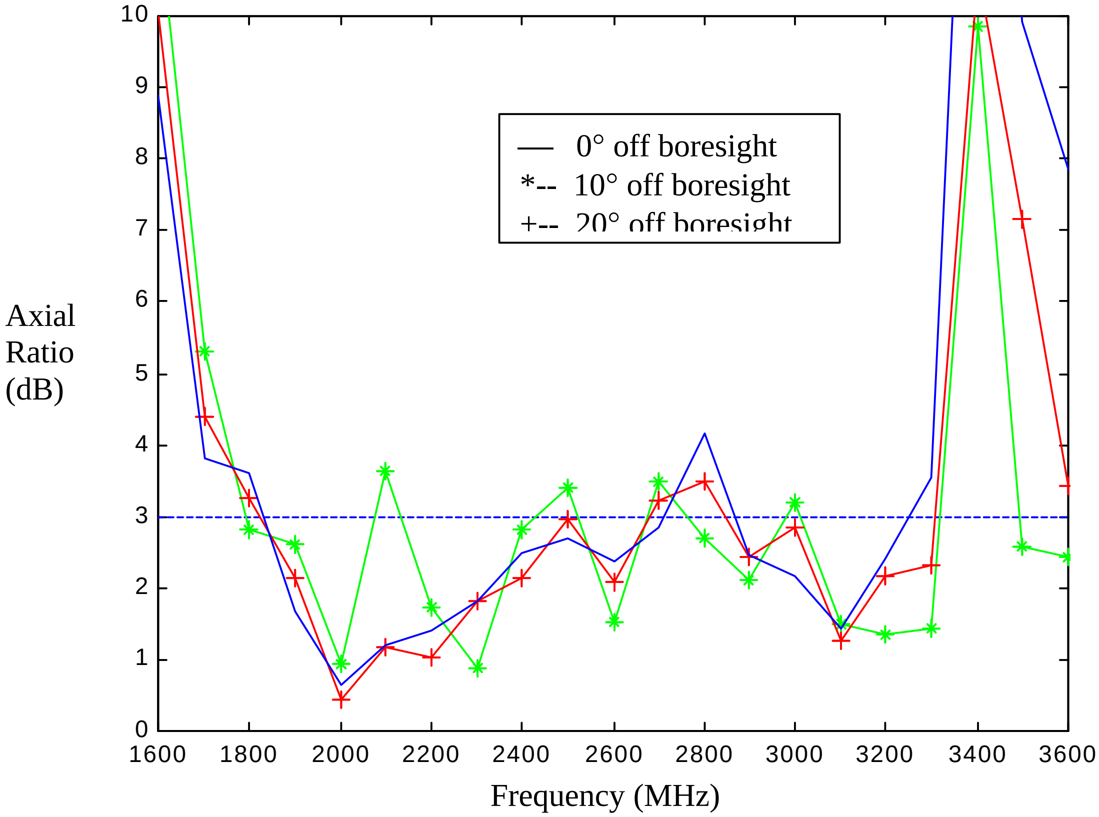

Figure 6.15 Measured axial-ratio at 0°, 10°, and 20° off of the boresight of the built GA-optimized helix.

6.4 Final Note

The antenna that was built and tested used a pie pan as the ground plane. Originally it was hypothesized that this shape would not adversely affect the pattern because the diameter of the pan is more than 1.5 wavelengths across. According to the early work by Kraus [18], a ground plane should be greater than 0.75λ. Thus, the pie pan was considered large enough so that the upturned sides would not greatly affect the patterns. It turns out that the up turned sides do affect the patterns.

Larger cone-shaped ground planes have been used in the past to reduce sidelobe levels and decrease the beamwidth of the helical antenna [21]. The upturned side of the pie pan does increase the gain slightly over a flat ground plane. Unfortunately the near field effects of the pie pan influence the pattern in different ways at different frequencies. At higher frequencies the pattern broadens out further than expected and the gain falls off.

In general, the use of a cupped ground plane increases the gain of a helical antenna. This project used an infinite ground plane while optimizing the helical structure because of the computing time constraints. Therefore, in order to see the results that are predicted in Figure 6.5, it is suggested that a sufficiently large and flat metal plate be used for the ground plane.

Chapter 7 Conclusions

The optimization of helical antennas using genetic algorithms was addressed. The basic concepts and variations of the genetic algorithm were reviewed. The genetic algorithm has proven to be a viable optimization technique that is perfectly suited for use in wire antenna design.

The helical antenna was chosen for this study because it does not have an analytical solution and therefore requires a numerical code to solve for the radiation fields. Numerical solvers do not provide insight into the optimal design for gain, axial- ratio or bandwidth, and therefore requires some type of optimization scheme. The genetic algorithm was used to design a helix that improves the gain, axial-ratio and bandwidth.

The use of NEC2 as the fitness function was tested in two ways. First, the results given by NEC2 were compared with known literature. Second, the GA-optimized helix was built and tested on the Virginia Tech antenna range. Both of these tests yielded acceptable results that proved that GA in conjunction with NEC2 is an acceptable optimization technique.

The GA-optimized helix provides an excellent axial-ratio performance. It has a higher gain, lower axial-ratio and wider bandwidth than a conventional helix. It was also shown that a GA-optimized helix that is half the size of a conventional helix with similar performance characteristics is possible.

7.1 Summary of Results

The important results of the study of the genetic algorithm and its use in designing an optimum helical antenna is presented below:

- The genetic algorithm is capable of optimizing wire antenna designs by using a moment method code such as NEC2 as the fitness function.
- The genetic algorithm should be used with $0.6 < p_{cross} < 0.9$ and $0.001 < p_{mut} < 0.01$. Tournament selection works best to properly converge the population while maintaining diversity. Elitist strategy should be used to maintain a monotonically increasing population fitness.
- The GA-optimized helix achieves higher gain, lower axial-ratio, a more constant input impedance, and wider bandwidth than the conventional helix. The axial-ratio performance of the GA-optimized helix is exceptional.
- The GA-optimized helix achieves a higher gain and wider bandwidth with increasing number of turns than the conventional helix. This is because the GA-optimized helix covers a range of pitch angles and therefore the number of turns does not effect the pitch angle very much. Increasing the number of turns merely increases the total wire length and therefore lowers VSWR and increases gain.
- The GA-optimized helix can achieve similar performance to the conventional helix with half the size.

7.2 Recommendations for Future Work

The genetic algorithm is a very robust optimization scheme that provides the opportunity to study many antenna designs. This thesis merely touches the surface of what the GA is capable of producing. Increasing the numbers of variables or giving the GA more freedom to discover unique designs can provide many new wire antenna designs.

As with all optimization techniques, time is the most important of all constraints. Using the genetic algorithm greatly improves the expense of the time required to root out an optimal solution. Still, there are many paths to follow to find better designs more rapidly. The follow is a list of suggestions for future work.

- The genetic algorithm has to evaluate a series of time consuming fitness functions. Evaluating the fitness function in parallel by using a network of computers or parallel processing would significantly decrease the time required. Using M computers would decrease the computation time by a factor of M.
- Exploring the many variations on the genetic algorithm such as evolutionary programming may turn up improved algorithm designs.
- By optimizing the helix design while using a finite ground plane similar to the one used to actually build the antenna would result in a design that is more accurate. This of course would be very time consuming.
- While the pitch angle changes with respect to the varying circumference, allowing the pitch angle to vary independent of the polynomial yield a better performance.
- Allowing a larger polynomial or some other type of envelope for the helix may result in a better performance.
- Other helical antenna designs such as spherical helices and spiro-helical antennas could be optimized using the GA.

References

1. J. H. Holland, *Adaptation in Natural and Artificial Systems.* Ann Arbor, MI: Univ. Michigan, 1975.
2. G. J. Burke, A. J. Poggio, *Numerical Electromagnetics Code (NEC) – Method of Moments*, UCID 18834, Lawrence Livermore Laboratory, 1981.
3. N. Patwari, A. Safaai-Jazi, "Predictions and Measurements of Double-Vee Dipoles," *AP-S Int. Symposium*, 1998, vol. 3, pp. 1426-1429.
4. D. E. Goldberg, *Genetic Algorithms in Search, Optimization and Machine Learning.* Reading, MA: Addison-Wesley, 1989.
5. C. Darwin, *The Origin of Species*, London, U.K.: Penguin 1985.
6. Y. Rahmat-Samii and E. Michielssen, *Electromagnetic Optimization by Genetic Algorithms*, New York: John Wiley & Sons, Inc., 1999.
7. R. L. Haupt, "Thinned Arrays Using Genetic Algorithm," *IEEE Trans. on Antennas and Propag.*, vol. 42, no. 7, July 1994.
8. K. Yan and Y. Lu, "Sidelobe Reduction in Array-Pattern Synthesis Using Genetic Algorithm," *IEEE Trans. on Antennas and Propag.*, vol. 45, no. 7, July 1997.
9. E. E. Altshuler and D. S. Linden, "Wire-Antenna Designs Using Genetic Algorithms," *IEEE Antennas and Propag. Magazine*, vol. 39, no. 2, April 1997.
10. D. S. Whiele, E. Michielssen, "Genetic Algorithm Optimization Applied to Electromagnetics: A Review," *IEEE Trans. on Ant. and Prop.*, vol. 45, no. 3, March 1997.
11. J. Holland, "Genetic Algorithms," *Scientific American*, July 1992, pp.66-72.
12. J. M. Johnson, Y. Rahmat-Samii, "Genetic Algorithms in Engineering Electromagnetics," *IEEE Ant. and Prop. Magazine*, vol. 39, no. 4, August 1997.
13. R. L. Haupt, "An Introduction to Genetic Algorithms for Electromagnetics," *IEEE Ant. and Prop. Magazine*, vol. 37, no. 2, April 1995.
14. G.A. Thiele, E.P. Ekelman, "Design Formulas for Vee Dipoles," *IEEE Trans. on Ant. and Prop.*, vol. AP-28, no. 4, July 1980, pp.588-590.

15. W.L. Stutzman, G.A. Thiele, *Antenna Theory and Design*. New York: John Wiley & Sons, 2nd ed., 1998.

16. R.E. Collin, *Field Theory of Guided Waves,* McGraw-Hill: New York, 1960.

17. J. A. Marsh, "Measured Current Distributions on Helical Antennas," *IRE Proc*., vol. 39, June 1951, pp.668-675.

18. J. D. Kraus, *Antennas*, 2nd ed., McGraw-Hill, New York, 1988.

19. H. E. King and J. L Wong, "Characteristics of 5- to 35-Turn Uniform Helical Antennas," Aerospace Corp. Tech. Rep. TR-0078(3724-01)-2, DDC AD A046487, June 1997; or "Characteristics of 1 to 8 Wavelength Uniform Helical Antennas," *IEEE Trans. Antennas Propagat.*, vol. AP-28, March 1980, pp.291-296.

20. T. S. M. Maclean and R. G. Kouyoumjian, "The Bandwidth of Helical Antennas," *IRE Trans. Antennas Propagat.*, vol. AP-7, special supplement, December 1959, pp. S379-386.

21. H. R. Carver, "The Helicone – A Circularly Polarized Antenna with Low Sidelobe Level," *Proc. of IEEE*, vol. 55, no. 4, April, 1967, pp. 559.

22. J. L. Wong and H. E. King, "Broadband Quasi-Taper helical Antennas," *IEEE Trans. Antennas Propagat.*, vol. AP-27, January 1979, pp72-78.

23. H. Nakano, J. Yamauchi, and H. Mimaki, "Tapered Balanced Helices Radiating in the Axial Mode," *Dig. Int. Symp. Antennas Propagat.*, 1980, pp. 700-703.

24. J. L. Wong and H. E. King, "Broadband Helical Antennas," U.S. Patent 4,169,267, September 25, 1979.

25. A. Safaai-Jazi and J. C. Cardoso, "Radiation Characteristics of a Spherical Helical Antenna," *IEE Proc. Microw. Antennas Propat.*, vol. 143, no. 1, February 1996.

26. R. M. Barts and W. L. Stutzman, "A Reduced Size Helical Antenna," *IEEE Antennas and Propagat. Society International Symposium*, 1997 digest, pp. 1588-1591, 1997.

27. P. D. Richeson. *NEC-2 User's Guide*. http://www.dec.tis.net/~richsop/nec

28. D. T. Emerson, "The Gain of the Axial-Mode Helix Antenna," National Radio Observatory, *Antenna Compendium*, Vol. 4, pp 64-68, 1995, http://ourworld.compuserve.com/homepages/demerson/helix.htm.

29. W.L. Stutzman, *Polarization in Electromagnetic Systems*. Massachusetts: Artech House, Inc., 1993.

Appendix

The following is the MATLAB code that was used to discover the GA-optimized helix. NEC2 was used to evaluate the helix structure and the fitness function assigned to each design is defined in HELIX_BW_INTERSECT.m.

```
% |Genetic Algorithm to find solutions:
% |    GA-optimized HELIX ANTENNA


clear
fclose all;

% |Variables


n = 3;       %number of variables
M = 8*n;     %Number of bits in chromosomes
N = 2*M*n;     %Number of chromosomes


PCross = .7;   %probability of crossover (mating)
PMut = .01;    %probability of mutation
decptN = 8;
decptr = -3;
counter = 0;
copyGF = zeros(1,M+1);   %Keep copies of previously run
solutions

copyfound = 0; %keeps track of whether a copy was found
NecRunCounter = 0;
```

```
order = 2;     %order of polynomial
freq = 2000;      %in MHz
lambda = 2.998e8/(freq*1e6);   %wavelength
h = 2*lambda;
z = [0:h/2:h];

%KEEP number of turns constant
Td = 12;

cc = 0;
%for test =1:20

%reset the clock timer
tic;
g = 0;


%First generate our initial population.
%CONSTRAINTS:
%  3 < N < 20
%  average f(z)=lambda/2*pi
minR = .01*lambda;
maxR = .25*lambda;


for j = 1:N

   %generate initial r's
   for i = 1:3
      r(i,:) = round( rand(1,M/n) );
      rd(i) = bin2decimal( r(i,:) , decptr );

      while (( rd(i) > maxR)|( rd(i) < minR ))
         r(i,:) = round( rand(1,M/n) );
         rd(i) = bin2decimal( r(i,:) , decptr );
      end
   end

   p = polyfit(z,rd,order);

   %average circumference
   circum = 1/h*( p(1)*h^3/3 + p(2)*h^2/2 + p(3)*h );
```

```
   while ( circum < .3*lambda/(2*pi) ) | ( circum >
2*lambda/(2*pi) )

      %generate initial r's
      for i = 1:3
         r(i,:) = round( rand(1,M/n) );
         rd(i) = bin2decimal( r(i,:) , decptr );

         while (( rd(i) > maxR)|( rd(i) < minR ))
            r(i,:) = round( rand(1,M/n) );
            rd(i) = bin2decimal( r(i,:) , decptr );
         end
      end

      p = polyfit(z,rd,order);
      %average circumference
      circum = 1/h*( p(1)*h^3/3 + p(2)*h^2/2 + p(3)*h );
   end
   g(j,1:M) = [ r(1,:) r(2,:) r(3,:) ];

end



% |Evaluate Fitness of Population
% |This is the initial testing of the Fitness function (f)

%The first set is always copied into the copyGF variable
%Td = bin2decimal( [0 0 0 g(1,4:M/n)], decptN );
for j = 0:order
   rd(j+1) = bin2decimal( g(1,j*M/n+1:(j+1)*M/n), decptr);
end

f(1) = helixrun_bw_intersect(rd, Td, h, order);
NecRunCounter = NecRunCounter + 1;
copyGF(1,:) = [ g(1,:) f(1) ];
[counter 1 f(1)]

for i = 2:N
   %First search through the copyGF var and see if this member
has already been
   %fitness tested.  If it has, simply use the same fitness
result instead of
   %re-evaluating the time consuming fitness function
   for j = 1:size(copyGF,1)
```

```
      if ( g(i,:) == copyGF(j,1:M) )
         f(i) = copyGF(j,M+1)
         copyfound = 1;
      end
   end

   %if there wasn't a copy found, evaluate the fitness function
and make
   %a copy of it in copyGF
   if ( copyfound ~= 1 )
      %Td = bin2decimal( [0 0 0 g(i,4:M/n)], decptN );
      for j = 0:order
         rd(j+1) = bin2decimal( g(i,j*M/n+1:(j+1)*M/n), decptr);
      end
      f(i) = helixrun_bw_intersect(rd, Td, h, order);
      NecRunCounter = NecRunCounter + 1;
   end
   copyGF(size(copyGF,1)+1,:) = [ g(i,:) f(i) ];
   copyfound = 0;
   [counter i f(i)]
   save helix_continue;
end


% |Start the loops to find the answer
stop = 0;

while ( stop == 0 )

   % |Elitist Strategy:  Find the best member and make
absolutely sure that
   % |he or she (grin) passes through to the end.  This
guarantees a monotonically
   % |increasing solution.  Check at the end for this elite
member.

   Best = 1;
   for j = 1:N
      if ( f(j) > f(Best) )
         Best = j;
      end
   end
   BestMember = [ g(Best,:) f(Best) ];
```

```
   % |Tournament Selection.  This selects N individuals at
random
   % |and the person with the highest fitness is selected.  This
   % |is continued until the population is refilled.

   gnew = zeros ( N,M );
   SetSize = 4;

   for i = 1:N

      RandSet = randperm(N);

      BestFit = RandSet(1);
      for j = 1:SetSize
         if ( f(RandSet(j)) > f(BestFit) )
            BestFit = RandSet(j);
         end
      end

      gnew(i,:) = g(BestFit,:);

   end

   g = gnew;


   % |Crossover  (Mating)
   % |This is used to mate the genes.  There is a PCross chance
that
   % |two random genes will mate.

   %   index = randperm(N);  %Used to do a random sorting
(random mating)

   for i = 1:2:N
      if ( rand < PCross )
         k = ceil((M-1)*rand);   %Used as a random place to
select the crossover point
         gnew(i,:) = [ g(i,1:k) g(i+1,k+1:M) ];
         gnew(i+1,:) = [ g(i+1,1:k) g(i,k+1:M) ];
      else
         gnew(i,:) = g(i,:);
         gnew(i+1,:) = g(i+1,:);
      end
   end
```

```
   g = gnew;

   % |Mutation
   % |This will occur only with a probability of Pmut (rarely)

   for i = 1:N
      if (rand < PMut)
         gmut = g(i,1:M);
         k = ceil((M-1)*rand);
         gmut(k) = 1 - g(i,k);

         g(i,1:M) = gmut;
      end
   end


   % |Evaluate Fitness of Population
   for i = 1:N

      %First search through the copyGF var and see if this
member has already been
      %fitness tested.  If it has, simply use the same fitness
result instead of
      %re-evaluating the time consuming fitness function
      for j = 1:size(copyGF,1)
         if ( g(i,:) == copyGF(j,1:M) )
            f(i) = copyGF(j,M+1);
            copyfound = 1;
         end
      end

      %if there wasn't a copy found, evaluate the fitness
function and make
      %a copy of it in copyGF
      if ( copyfound == 0 )
         %     Td = bin2decimal( [0 0 0 g(i,4:M/n)], decptN );
         for j = 0:order
            rd(j+1) = bin2decimal( g(i,j*M/n+1:(j+1)*M/n),
decptr);
         end
         f(i) = helixrun_bw_intersect(rd, Td, h, order);
         NecRunCounter = NecRunCounter + 1;
         copyGF(size(copyGF,1)+1,:) = [ g(i,:) f(i) ];
      end
```

```
      copyfound = 0;
      [counter i f(i)]
      save helix_continue;
   end


   % |Elitist check.  If no member is as good or better than the
original
   % |elite member, randomly replace one of the members with
this elite member.

   if ( max(f) < BestMember(M+1) )
      i = ceil( (N-1)*rand );
      g(i,:) = BestMember(1:M);
      f(i) = BestMember(M+1);
   end


   %keep looping until there is no difference in members of
population
   if ( std( f ) < 0.001 )
      stop = 1;
   end

   counter = counter + 1;
   fsave(counter,:) = f;
end

%*************************************************************
*****%
%*************BIN2DECIMAL.m***********************************
*****%

% |convert binary string to decimal
% |usage: dec = bin2dec( binary, M )
% |M is the decimal point placement

function dec = bin2decimal( binary, M )

dec = 0;

for i=1:length(binary)
   dec = dec + binary(i).*2^(M-i);
end
```

%**
****%
%*******
HELIX_BW_INTERSECT.m**%

```
%FITNESS FUNCTION!
%Find the intersection of the BWg and the BWar

function BW = helixrun_bw_intersect( r, N, h, order )

%| 1.  Set up constants

freq =2000;   %in MHz
lambda = 2.998e8/(freq*1e6);
order = 2;
z = [0:h/order:h];

p = polyfit(z,r,order);


  rad    = 0.0005;
  dtheta = 180;
  dphi   = 180;
  prefix  = 'helix';
  infile  = sprintf('%s.dat',prefix);
  outfile = sprintf('%s.out',prefix);
  seg_turns = 25;
  segments = 1;    %number of segments to split up each piece
into

 init_h = .05*lambda;


  %| 2.  Create the variable helix file and run NEC
  [wd] = helixdata(p,h,N,seg_turns,init_h);
  helixdatfile(infile,wd,rad,dtheta,dphi,segments,freq);
  [s,w] = dos(sprintf('nec2d1k4 <infile' ));
```

```
%This D is for center freq, 1e3 Mhz.

[D,AR] = getDandAR(outfile);


if ( ( D >= 9 )&( AR > .707 ) )

   freqr = freq;
   freql = freq;

      freqr = freqr + 50;
      helixdatfile(infile,wd,rad,dtheta,dphi,segments,freqr);
      [s,w] = dos(sprintf('nec2d1k4 <infile'));
      [D2r,AR2r] = getDandAR(outfile);

      freql = freql - 50;
      helixdatfile(infile,wd,rad,dtheta,dphi,segments,freql);
      [s,w] = dos(sprintf('nec2d1k4 <infile'));
      [D2l,AR2l] = getDandAR(outfile);


   %test right side
   while ( ( AR2r > .707 )&( AR2l > .707 )&( D2r > D-3 )&( D2r
<= D )&( D2l > D-3 )&( D2l <= D ) )
      freqr = freqr + 50;
      helixdatfile(infile,wd,rad,dtheta,dphi,segments,freqr);
      [s,w] = dos(sprintf('nec2d1k4 <infile'));
      [D2r,AR2r] = getDandAR(outfile);

      freql = freql - 50;
      helixdatfile(infile,wd,rad,dtheta,dphi,segments,freql);
      [s,w] = dos(sprintf('nec2d1k4 <infile'));
      [D2l,AR2l] = getDandAR(outfile);
   end


   Bandwidth = freqr-freql;
   BW = Bandwidth + D;%10^(D/10)*Bandwidth;

end

if ( ( D < 9)|( AR < .707 ) )  BW = 0;
end
```

Vita

Raymond Lovestead was born to Li-Ming and Leslie Lovestead in 1975 in Balboa, Panama. He graduated from Robert E. Lee High School in Springfield, Virginia in 1993. He attended the Virginia Polytechnic Institute and State University and received his Bachelor of Science degree in electrical engineering in 1997. He continued on at Virginia Tech for his Masters in the electrical engineering department. The bulk of his studies concentrated on communications and electromagnetics as applied to antennas. He received his Masters of Science in October 1999. Raymond Lovestead currently lives with his wife, Tara, in Boulder, Colorado. His wife is pursuing her Ph.D. in chemical engineering.